Modeling Strong Discontinuities using Generalized Finite Element Method (GFEM)

Mahendra Kumar Pal

A Dissertation Submitted to

Indian Institute of Technology Hyderabad

In Partial Fulfillment of the Requirements for
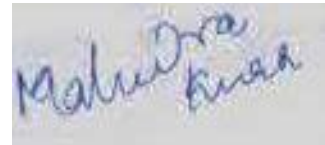
The Degree of Master of Technology

भारतीय प्रौद्योगिकी संस्थान हैदराबाद
Indian Institute of Technology Hyderabad

Department of Civil Engineering

Indian Institute of Technology Hyderabad

June, 2012

Declaration

I declare that this written submission represents my ideas in my own words, and where others ideas or words have been included. I have adequately cited and referenced the original sources. I also declare that I have adhered to all principles of academic honesty and integrity and have not misrepresented or fabricated or falsified any idea/data/fact/source in my submission. I understand that any violation of the above will be a cause for disciplinary action by the Institute and can also evoke penal action from the sources that have thus not been properly cited, or from whom proper permission has not been taken when needed.
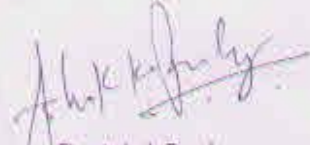
(Signature)

Mahendra Kumar Pal

(----- Student Name --)
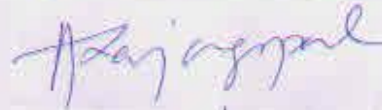
CE10M06

(---Roll No--)

Approval Sheet

This thesis entitled "**Modeling strong discontinuities using Generalized Finite Element Method**" by **Mahendra Kumar Pal** is approved for the degree of Master of Technology from IIT Hyderabad.

Dr. Ashok Pandey
Examiner

Dr. KVL. Subramaniam
Member

Dr. A. Rajagopal
Advisor & Chairman

Acknowledgements

I would like to praise and thanks to almighty GOD for his gift to me as wisdom and knowledge. He conferred the intelligence to me for endeavoring in my research work.

I would like to convey my special thanks to my thesis advisor Dr. A. Rajagopal for all his faith and confidence in me. He believed in me and given such an awesome topic to work on it. Working with him and being a part of his research group is privilege for me. It would have been highly impossible for me to move forward without his motivation and well organized guidance. His encouragement and technical guidance made my thesis work worth full and interesting. I can never repay the valuable time that he had devoted to me during my thesis work. Working with him was indeed a fantastic, fruitful, and an unforgettable experience of my life.

I am also indebted to say my heartily thanks to my Head of Department, Prof. K.V.L.Subraminam for the confidence in me that he always shown. It gives me immense pleasure to thank my faculty members who taught during my M.Tech course work. I would like to thank Prof. M.R. Madhav, Dr. B. Umashakar, Dr. S. Sireesh for their valuable suggestion during my course work.

I am thankful to my prestigious institute Indian Institute of Technology, Hyderabad for all the support and providing everything whatever was required for my research work.

I am grateful and thankful all my friends. I would like to say special thanks to my supervisor's research group members L. Harish (M. Tech.), B.Umesh (PhD.), Balakrishana (PhD.), Nitin Kumar (M.Tech.), KS.Balaji (M.Tech.), S. Madhukar (Project Associate).

Dedicated to

My parents and my sweetest sister

Abstract

Computational modeling of strong discontinuities is a challenging a task. Stress analysis and shape sensitivity can be done with any simulation method such as finite element method, finite difference method, Rayleigh-Ritz method, weighted residual method or least square method. All these numerical analysis methods are computationally expensive and uneconomical. Mesh dependency with respect to fracture boundary is a major problem in these methods. Furthermore accuracy of the methods depends on the size of the discretized element.

To bring the mesh independency the classical FE approximation is extended or enriched. This enrichment gives a higher order approximation and better reproducibility of the field ahead of the crack tip. The developed method requires a very less computation space and is also an economical method for complex problems. This proposed method is called as extended finite element merthod (XFEM).

The Generalized Finite Element Method (GFEM) is based on the enrichment of the classical approximation. The enriched basis is achieved with the help of the various enrichment functions. These enrichment functions are capable to mimic the presence of the crack boundary, dislocation or discontinuity in the domain. These functions are selected on a priori knowledge of the solution of the given problem. Different enriched basis function has been demonstrated for demonstrating the capability of the GFEM.

In the present work GFEM is presented as a potential methodology for modeling the complex geometries and fracture problems. Methodology is implemented to assess the true strength, durability and the integrity of the structure/ structural components. The interdependency of the input variables and their effect on the output has been studied in the sensitivity analysis. During the implementation of the methodology various issues like inter-boundary conflict for the different approximations, numerical integration of the crack domain, assembly of the global stiffness matrix,

and numerical instability of the global stiffness matrix have been suitably addressed. These issues have been explored and rectified with efficient and optimal method.

Structural optimization plays the key role in the design industry. Prediction of the fatigue life and strength of the structure is another important factor of this industry. Fatigue life and the strength depend on the various independent and dependent variables. It's a challenging task to identify the important variable in the design. This objective can be easily achieved with the shape sensitivity analysis of the any fracture parameter such as stress intensity factor (SIF), J-integral. We have studied the shape sensitivity of the J-integral. Results show the dependency of the J-integral on the various conditions as well as on variables.

In order to demonstrate the potential of the method, an edge crack problem has been considered an example. Elastic and hyper-elastic cases are considered for analysis. Sensitivity analysis has been illustrated for same geometry numerical problem. Sensitivity analysis has been performed with different boundary and loading conditions. Effect of crack length on the J-integral has been illustrated. The sensitivity analysis is based on the variational formulation of the continuum mechanics. A bimaterial domain has been also taken as another example for sensitivity analysis. Mathematically sensitivity analysis is defined as the differentiation of that entity with respect to the independent variable. This definition has been used for validation of the results. This alternative approach is based on the first principle of the differentiation.

Nomenclature

N_i Classical shape function

$\emptyset_k$ Enrichment function

$\emptyset_{1,r}$ Derivative of enrichment function

u_i Classical Nodal freedom

b_1 Additional Nodal freedom

H Heaviside function

r and θ Polar coordinate system near the tip

Γ_t Traction Boundary

Γ_u Displacement Boundary

Γ_c Cracked Boundary

σ 1$^{\text{st}}$ order stress tensor

f^b Body force

f^t Applied Traction

$\bar{u}$ Prescribed Displacement

Ω Domain

W Work done and strain energy

B_i^a Shape function derivative matrix

K Stiffness matrix

f_i^e Vector of element external force

K_I Stress intensity factor for Mode-I

K_{II} Stress intensity factor for Mode-II

K_{III} Stress intensity factor for Mode-III

J J-Integral

$d(x)$ Distance function

$R(x)$ Blending function

λ and μ Lame's parameters

$\bar{I}_1$ and $\bar{I}_2$ First and second invariant of the unimodular component of the left Cauchy-Green Deformation tensor

C_{ijkl}	Material response tensor of 4th order
g_{ij}	Material response tensor of 2nd order
$T(x,\tau)$	Transformation mapping
$V(x,\tau)$	Velocity field
$\dot{u}(x)$	Material derivative of displacement field
$\dot{J}$	Material derivative of J-Integral
G_i	Sensitivity function
g	Sensitivity function
E	Young's Modulas
G	Bulk Modulas
δ	Prescribed displacement
$L * B$	Length* width

Contents

Chapter 1

Introduction

1.1 Motivation

The Finite Element Method (FEM) has been found wide used of enormous application in many fields. FEM approximation is interpolatory in nature. This interpolatory nature of approximation in FEM makes the solution mesh dependent. One possibility to achieve accuracy in solution is by adaptive refinement of mesh. However such schemes are computationally expensive. FEM does not suit well to treat problems with discontinuities (i.e. Crack propogation) that do not align with the mesh. Meshless Methods (MMs) have been used with objective of eliminating part of difficulties associated with reliance on mesh to construct the approximation. MMs are based on approximations that are not interplatory in nature but are based on alternative strategies like for instance the moving least square (MLS) approach. The problem associated with these methods is that they are computationally expensive and non interpolatory nature requires Lagrange multipliers for imposition of boundary conditions.

There has been a need for developing better approximation schemes that have interpolatory characteristics, consistency and stability. Also in using such methods for fracture problems, the methods should be capable of reproducing the actual stress/ strain field ahead of the crack tip. To this end, there has been many works on improving the classical FEM approximations and one such methodology was coined as Extended Finite Element Methods (XFEM). In these methods the approximation is enriched by some additional enrichment functions. However there were difficulties associated with the method as regards making appropriate choice on the enrichment functions.

Minimizing the error between approximation solution and exact solution can make appropriate choice on the enrichment functions belonging to a particular function space. Proper Orthogonal Decomposition (POD) is done on the fact that distance between member of ensemble and subspace is minimal. An XFEM with choice on enrichment functions based on POD is termed as Generalized Finite Element Method (GFEM) [10].

In this work POD has been used for finding out the enrichment basis function for GFEM approximation [10]. Such a enrichment function accounts for the oscillatory nature of the solution ahead of singular regions. The global approximation has been constructed by combining the local bases with partition of unity functions (i.e. classical basis function).

1.2 Outline of Thesis

The thesis has been divided into the 9 chapters. The first chapter contains the motivation and second chapter contains the literature survey of XFEM/GFEM. Third chapter contains the review of fracture mechanics. Realization of the capability of GFEM has been illustrated through the shape functions in 1-D and 2-D in the following chapter. Different examples of enrichment functions have been demonstrated in this chapter. Two scales GFEM has two different orders of the approximation, which results into the inter-boundary conflict for the neighboring elements to enriched elements. The blending element concept has been introduced to ensure the continuity among the two different approximations. Next chapter continues the discussion about the blending element. Fourth chapter contains the mathematical foundation of Galerkin formulation of the GFEM and the numerical integration schemes respectively. This chapter also contains the discussion over the implementation issues of the GFEM. Stress analysis of the fracture problems has been shown in the seventh chapter. Eighth chapter contains the sensitivity analysis of the edge crack problem. Final chapter ends with a conclusion and the Scope of the future work.

Chapter 2

Literature Review

2.1 Choice of Enrichment Function in XFEM/GFEM

A Judicious choice is required to be made in the selection of enrichment function. The main objective of enrichment function is that it should able to reproduce the singular stress field near crack tip. Selection of enrichment function is done by apriori knowledge of solution. XFEM and meshless methods have used the partition of unity enrichment for solving the crack problems. Belytschko et al. [7] described methods based on the partition of unity for approximating discontinuous functions in finite element and meshless formulations. Fries and Belytschko [8] presented a new intrinsic enrichment method for treating arbitrary discontinuities in a FEM context. Unlike the standard XFEM, no additional unknowns were introduced at the nodes whose supports were crossed by discontinuities. An approximation space was constructed consisting of mesh based, enriched moving least squares (MLS) functions near discontinuities and standard FE shape functions elsewhere. Belytschko and Black [1] introduced a method for solving crack problem in finite element framework. In this method the meshing task is reduced by enriching the element near the crack tip and along the crack face with leading singular crack tip asymptotic displacement fields using partition of unity method to account for the presence of crack. Enrichment function need not be known solely in closed framework but results from numerical simulation can be used as enrichment functions. Later authors used canonical domain containing features such as branched cracks, or closely spaced voids to generate what they called mesh-based handbook functions. This approach is very useful for the situations in which analytical expressions, which reflect the nature of solutions, are not available. For enrichment in the introduction paper of GFEM, Strouboulis [4] had used harmonic function as enrichment function to enrich the basis of approximation. Aquino et al [10] had shown that due to appealing approximation properties, POD modes are best choice of the enrichment function in the GEFM. For a proper orthogonal decomposition – Generalized finite element method (POD-GFEM) formulation, the POD modes $\varphi_p(\mathrm{x})$ are used as the enrichment functions in Equation (1). GFEM basis function is union of the classical finite element polynomial basis $\{N_i\}^s_{i=1}$, and the enriched

bases, $\{N_i \varphi_p\}_{i=1}$ $(p = 1,2,3 \ldots\ldots, m)$. where s is number of nodes and m is the enrichment functions (POD modes). This has been used in the present work

$$u^h(x) = \sum_{i \in I} N_i(x) u_i + \sum_{\alpha} \sum_{j \in I} N_j(x) \emptyset_\alpha(x) a_{j\alpha} \qquad (2.1)$$

Where $\emptyset_\alpha$ is the enrichment function, I is total number of nodes, $a_{j\alpha}$ is the additional degrees of freedoms.

Mousavi et al [9] had proposed new enrichment function named as harmonic enrichment function. To model weak discontinuities in bimaterial interfaces, Moes et.al [11] proposed a ridge function. The ridge function is continuous across the interface, though the gradient of ridge function is discontinuous. The ridge enrichment is well suited for continuous deformation map and Moes et al [11] reported optimally convergent results in the small strain regime for linear elastic materials with relatively small modulus mismatch. Arndtl et al [12] had used generalized finite element method for vibration analysis of straight bars and trusses. They had used enrichment functions as combination of some trigonometric functions.

Along with selection of enrichment function, there are some issues, which appear in the evaluation of integrals over the element domain. Classical Gauss quadrature rules fails for discontinuous domain. Ventura [13] had shown the way that how classical gauss quadrature rule can be used for discontinuous domain by splitting the element into sub cells. Sunderrajan et. al [26] had proposed the numerical integration scheme based on conformal mapping. Convergence is main criterion to be satisfied for any kind of method. Labordr et al [14] and Chahine et al [15] has targeted the convergence and studied the convergence for variety of XFEM on cracked domain.

Numerical instability is a problem concerning solution in GFEM. These numerical instabilities come into the scenes due to the singular stress field ahead of crack tip. Peter and Hack [16] had discussed the ways that a singular stiffness matrix may be avoided by static condensation of row and column corresponding to some of the enhanced degree of freedoms. Xiao and Karihaloo [17] discussed improving the accuracy of XFEM crack tip fields using higher order quadrature and static admissible stress recovery procedures. The static admissible stress recovery scheme is constructed by the basis functions and Moving Least Square (MLS) to interpolate the stress at integration points obtained by XFEM.

XFEM has been widely used in field of multiscale modeling of the material. In multiscale modeling different level of accuracy is required which varies from atomic level to macro simulation level. Since GFEM approximation has ability to reproduce multiscale effects in modeling so many of the researchers have used GFEM technique for multiscale modeling. Hirari et. al [18] had proposed zooming technique with local global approximation which enhance the classical FEM over the entire region of domain. In this technique mesh was refined on the critical region (i.e. stress concentration region). In a superposition multiscale approach, global and local

parts are modeled independently, and then superimposed to provide the final solution by satisfying the compatibility equations. Haider et. al [19] has proposed homogenization based multiscale modeling which is based on domain decomposition technique. In this technique domain is divided into several sub domains, which are connected by the interface element.

2.2 Review of XFEM applications

Many of the engineering problems had been analyzed using the XFEM. A few of them has been discussed here. The methodology for multiple and arbitrary crack propagation problem had been proposed by Areias and Belytschko [20] with enrichment of rotation field. Areiase et. al [21] had proposed the very similar formulation as Hansbo and Hansbo [22] did for the evolution of crack in thin shells using mid surface displacement and director field discontinuities.

XFEM has been explored for dynamic problems by Belytschko et. al [23], Belytschko and Chen [24], and Zi et. al [25] which are based on singular enrichment FEM. Rathore et al [26] proposed GFEM to model dynamic fracture with incorporating time dependency. Menouilllard et. al [27] published a paper on explicit XFEM. In this publication they have introduced lumped mass matrix for enriched element.

XFEM has been wide application for coupled problems. Chessa and Belytschko [28, 29] published and proposed a methodology for solving hyperbolic problems with discontinuities based on a locally enriched space–time XFEM. The coupling was implemented through a weak enforcement of the continuity of the flux between the space–time and semi-discrete domains in a manner similar to discontinuous Galerkin methods. Furthermore Rathoré et al. [30] proposed a combined space–time XFEM, based on the idea of the time extended finite element method, allowing a suitable form of the time stepping formulae to study the stability and energy conservation.

The feasibility of extending the traditional FEM to Generalized finite element method (GFEM) has been demonstrated by Strouboulis and Babuska [3]. The target had been achieved by adding special functions to the approximation. These special functions can be selected on the basis of available information about boundary value problems. The functions are combined with linear finite element hat functions, which follow the partition of unity and provide the flexibility in the approximation. The flexibility of GFEM means approximation space can be formed by any mixture of special local approximation functions at disposal. One can mix quadratic and higher order traditional polynomial basis function defined on master element. Strouboulis et. al [3] have chosen grids which are quasi uniform meshes typically used in standard FEM and used the regular Legendre shape functions with element degree two. He has assumed two combinations of special functions. In the first case, he starts with the uniform p-order tradition FEM shape functions $p_{FEM}=2$ and add one or more layer of singular function. This is called singular case. In second case he computed approximation in which he limits the FEM element degree to $p_{FEM}=1$ and added

5

successive terms. Using successive increasing terms in all special functions may give error comparable but no significant advantage in convergence is obtained beyond that provided by singular path space. This is because he used the singular patch only in the elements with vertex at the corner, if he may have increase the n layer i.e. use of special singular functions at vertices surrounding the corner, he may get a good convergence rate. In this study they have focused on the theory behind the new approximation and it was limited to the 2-dimensional problems.

At the same time Duarte et. al [5] had explored the same concept for three dimensional problems. Their works based on traditional h-p finite element method. They had used tetrahedral mesh and a priori knowledge of elastic solution to get the p-orthotropic approximation. They have improved the traditional h-p finite element method by using h adaptivity with the partition of unity. They had suggested using a polynomial basis function to build the approximation space. They had investigated the structure of stiffness matrix for its rank and size of matrix. They have calculated the strain energy and showed the applicability of the proposed algorithm.

After establishing the theoretical foundation of GFEM, Strouboulis et. al [4] had elaborated the it for the various applications. GFEM is mesh independent methodology and is based on optimal basis function.

During implementation they came up with some issues. The main issue in the GFEM came out as the integration as a classical Gaussian quadrature rule fails due to the presence of discontinuity. So to avoid this shortcoming, they had proposed the fast remeshing approach. In this approach they had divided the element into subdivision and named it as nested subdivision. This algorithm became the most essential tool for implementation of GFEM in fracture problem.

Second issue appeared as the decision on the selection of enrichment functions since Shape function of any methodology reflects the behavior of its approximation. Babuska et. al [31] had taken this issue and explained the principle for the selection of enrichment function. They had illustrated the   performance of various kinds of enrichment function such as a sine function, polynomial function and other trigonometric functions. They have made remarks on the order of the function through the asymptotic rate of convergence. They had illustrated the polynomial function by pre-asymptotic performance of approximation. They had concluded that shape functions are best available information about the approximation method. They had made remarks that enrichment function should characterize on the smoothness. In case of sobolev- type spaces the polynomial function is the best choice. They emphasized on the compact support ness of the basis function.

Another issue was realized as the inter-boundary approximation conflict. There is a jump between the enrichment approximation and classical approximation. Due to this jump between two approximations, there is degradation in the convergence rate. For increasing the computational efficiency blending function had been used for smoothing the approximation. This concept was introduced by Sukumar [52] and then it has been elaborated by Chessa et. al [32]. They had

introduced the enhanced strain methods, which is basically depends on the eliminating the unwanted terms in the approximation. They had assumed the strain as a summation of symmetric displacement gradient and an enhanced strain filed.

$$\bar{\varepsilon} = \vec{\nabla}u^h + \varepsilon^{enh}$$

(2.2)

Where $\bar{\varepsilon}$ is strain, $\vec{\nabla}u^h = Bd$ is displacement gradient

They had put the condition for discontinuous polynomial enrichment that blending element will give linear field if the following inequality holds.

$$s \geq e + p$$

(2.3)

Where s complete order of the function, e order of the shape function, p order of the polynomial enrichment function.

Performance of the developed tool can be increased either using the strain enhanced element for blending element or by using signed function with polynomial functions.

Babuska et. al [33] had presented the state of the art of GFEM as a review paper. In this paper they had briefly discussed about the main ideas, and various issues related to the GFEM. They had documented the mathematical foundation and the formulation of GFEM approximation. They have talked about the selection of the approximation spaces. Selection of the approximation function depends upon the following points

Available information on the elastic solution in terms of Sobolev spaces and boundary value problem is used for obtaining the enrichment function. Using these enrichment functions, they are making the decision for the order of the approximation. The decision for the selection of enrichment function also depends on the a priori knowledge of the solution. This decision is taken with preserving the conformal mapping of the complex geometries.

They have emphasized on the implementation portion of the GFEM and the issue related to the implementation. Finally they have concluded that GFEM is the best tool for problems with complex geometries and non-smooth solution. GFEM has potential of being used in context of mixed formulation.

Pereira et. al [34] has implemented the contour integral method to extract the SIF values from GFEM solutions. They had investigated the contour integral method, cutoff function method along with J-integral method for calculating the SIF values. They have studied the relative error variation with respect to the number of degrees of freedom, integration radius. Variation of SIF values (K_I and K_{II}) with respect to the number of degrees of freedom and integration radius had been demonstrated. They have made remarks that these parameters are sensitive to the extraction domain. Selection of extraction domain is an important decision in this method.

Realizing the potential of GFEM, Strouboulis et. al [35] has extended their work for solving the Helmholtz equation. In the proposed methodology they have used the plane wave function as the enrichment function. They have studied the pollution effects in the results. Pollution effects can

be defined as the deviation of Galerkin solution from the exact solution. They had studied the p and q convergence. q is the number of plane wave**s** added. They had talked about the implementation of the proposed methodology. Error follows the triangle's inequality

$$\left| \left\| |u - u_h^{p,q}| \right\| - \left\| |u_h^{p,q} - u_{h*}^{p,q}| \right\| \right| \le \left\| |u - u_{h,*}^{p,q}| \right\| \le \left\| |u - u_h^{p,q}| \right\| + \left\| |u_h^{p,q} - u_{h,*}^{p,q}| \right\| \qquad (2.4)$$

$\left\| |\boldsymbol{u}_h^{p,q} - \boldsymbol{u}_{h,*}^{p,q}| \right\|$ is the numerical integration error. They had used Gauss elimination with partial pivoting for solving the discrete system of equations. They had studied the relative error with respect to the number of degrees of freedom. It was observed that the pollution effect cannot be avoided and Convergence criterion has an exponential rate with respect to wave direction. Numerical integration is an important step in GFEM. One has to very careful in the calculation of the same.

In another work [36] choice of enrichment function and various kinds of errors are discussed in the solution. Pollution errors are directly dependent on the number of plane wave functions. Choice of handbook function affects the convergence of the approximation. But the choice of such function depends on the computation cost and ease of implementation. It does not affect convergence. Boundary conditions can also affect the accuracy of the solution, since they can couple with error from interior approximation and other dominant computing the errors. In this work they have studied the relative error with respect to the number of plane waves used in solving the system.

Duarte et.al [37] has an emphasized on the application of global –local enrichment function in 3-D fracture, which has been successfully used to construct an enriched basis for generalized FEM. Global-local enrichment function uses the same approach as used in global-local FEM. Fundamental difference, however, is that the proposed generalized FEM accounts for possible interaction of local (near crack for example) and global (structural) behavior. These interactions can be accounted when solving the global problem with global local enrichment functions. This is in contrast to standard global-local FEM.

This global-local enrichment approach is used to define following vector-valued global shape function

$$\phi_\alpha = \varphi_\alpha u_{loc} \qquad (2.5)$$

Where ϕ_α denotes a global partition of unity function. This function is used at nodes xα of the global mesh whose support, ω_α is contained in the local domain Ω_{loc}.

Let's u_G^0 denotes generalized FEM approximation of the solution of governing differential equation. The approximation is solution of following problem

Find $u_G^0 \in X_G^{\text{hp}}(\Omega_G) \subset \text{h}^1(\Omega_G)$ such that, $\forall v_G^o \in X_G^{\text{hp}}(\Omega_G)$

$$\int_{\Omega_G} \sigma(u_G^o) : \varepsilon(v_G^o) dx + \eta \int_{\Omega_G} u_G^o . v_G^o ds = \int_{\partial\Omega_G} \bar{t}.v_G^o ds + \eta \int_{\partial\Omega_G} \bar{u}.v_G^o ds, \qquad (2.6)$$

where $X_G^{hp}(\Omega_G)$ is a discretization of $h^1(\Omega_G)$, the Hilbert space defined on Ω_G, built with generalized FEM shape function and $\boldsymbol{\eta}$ is a penalty parameter

Srinivasan et. al [38] have presented the extension GFEM in the context of heterogeneous material. They have done hyperelastic analysis of bimaterial solid. In the proposed methodology, they have considered the approximation function as the summation of the classical and enriched displacement fields. They have considered the independent enrichment functions, which are decided on the basis of a priori knowledge of the solution field. These enrichment functions are linearly independent of each other.

$$u^{\text{h}}(x) = \sum_{i=1}^{n} \varphi_i(x) . u_i + \sum_{\alpha} \sum_{k=1}^{r} \psi_k a_{k\alpha} \qquad (2.7)$$

For demonstrating the proposed methodology, they have used Ridge function in place of classical Heaviside function. They have demonstrated the capability and robustness of the discontinuous deformation map formulation. Belytschko et. al [39] has presented a review paper entitled as A review of XFEM/GFEM for material modeling. In this publication they have mentioned about the capabilities and advances of the GFEM.

They had discussed the various kinds of the enrichment function. As the selection of the enrichment function depends on the priori knowledge of the solution. They have mentioned type of enrichment function depending on the type of the problem definition. These are tabulated in Table 1.

Table 2.1: Type of enrichment function and their use

S.No.	Type of Problem	Enrichment function
1	Crack / Fracture Problem	Heaviside function for crack +Level set function Crack- tip enrichment function for tip Level set function
2	Dislocation	Level set function Combined step and core enrichment function Step enrichment functions- for non-linear and anisotropic problem.
3	Grain Boundaries	Heaviside step function
4	Phase interface	Gradient of approximation function Ridge function or Tent function Signed distance function

In the current state of construction, our structures are becoming taller and taller. These taller structures are dynamically unstable. They may have vibration and other oscillation. Reason for these kinds of effects may be wind or earthquake force. Even water current force can also be a reason in the case of bridge pillar. Vibration analysis of such kind of structures is very tough and complicated to the implementation point of view. Arndt et. al [40] had illustrated the vibration analysis of the these kinds of tall structures. They had demonstrated the proposed methodology for a straight bar and trusses. In the study they have assumed the approximation function as a summation of classical approximation and the enriched approximation.

$$u^h(x) = u^{FEM} + u^{enriched} \qquad \text{(2.8 a)}$$

$$u^h(x) = \sum_{i=1}^{n} N_i u_i + \sum_{k=1}^{n} N_k(x)\left[\sum_{j=1}^{r} \psi_{kj}(x)a_{kj} + \phi_{kj}(x)b_{kj}\right] \qquad \text{(2.8 b)}$$

N_i is the classical shape function, ψ_{kj} and ϕ_{kj} are enrichment functions.

The enrichment functions for vibration analysis are as follows

$$\psi_{kj} = \sin(\beta_j L_e x)$$

$$\psi_{kj} = \sin\left(\beta_j L_e(x-1)\right)$$

$$\phi_{kj} = \cos(\beta_j L_e x) - 1 \qquad \text{(2.9)}$$

$$\phi_{kj} = \cos\left(\beta_j L_e(x-1)\right) - 1$$

Babuska et. al [41] had extended the GFEM work form fracture simulation to multiscale modeling. This work was done with the objective of optimal accuracy. An approximation error had been controlled with the help of local approximation. They had talked about the identifying the local approximation spaces. Then the optimal local approximation space is combined within the GFEM. These optimal local spaces have been used as the enrichment functions. The next question arises that how to find out the optimal local spaces. They had done some mathematically manipulations and shown that this is like an eigenvalue problem. Finding out the eigenvalues and corresponding eigenvector is an easy from an implementation point of view. Eigenvalues and corresponding vector can be found out using Singular value decomposition (SVD), Proper Orthogonal Decomposition (POD) or eigen value problem itself. They have developed a mathematical formulation for the homogenization problem. As an example they had considered the fiber reinforced composites, which is a typical example for multiscale modeling. They had discussed the associated approximation error.

2.3 Observations from literature review

Selection of these enrichment functions is still a challenging work which is usually done with the priori knowledge of solution. Here in this work we are using POD [10] basis function as enrichment function for our case. These basis functions can also be readily used for multiscale modeling. Numerical Integration is another challenging work to incorporate within the formulation. It's essential to use a very efficient and versatile integration scheme for evaluation of integrals over discontinuous domain. In this work we adopt an element partition method [13] for numerical evaluation of integrals. Blending element approximation is one more crucial deciding factor to be considered. For bringing the smoothness of approximation function over the all nodes of blending element, blending or ramp function has been used.

2.4 Objective and Scope of the Work

[1] To perform a state of the art review on XFEM/GFEM technique

[2] To study and incorporate various types of enrichment functions that will be helpful in developing enriched bilinear quadrilateral elements.

[3] To develop software for two scale modeling of strong discontinuities using GFEM that will be mesh independent and require no remeshing. The software will incorporate suitable quadrature scheme for numerical evaluation of integrals for each element.

[4] To demonstrate the working of the software through numerical experiments.

[5] To demonstrate the sensitivity analysis of the edge crack problem

The scope of the work is limited to

[1] Limited to linear elastic and Hyperelastic analysis for 2 dimensional problems.

[2] Limited to enrichment of bilinear element.

[3] Limited to static analysis of the fracture problems.

Chapter 3

Fracture Mechanics: A Bacground

3.1 Basics of fracture Mechanics

The study of the discontinuities or crack in material is important from various prospective viz. aerospace, machine design and concrete structures. In presence of crack the conventional theory of strength of material fails. In order to explain the difference in fracture mechanics and conventional strength of material, consider an example as shown in Fig. 3.1.

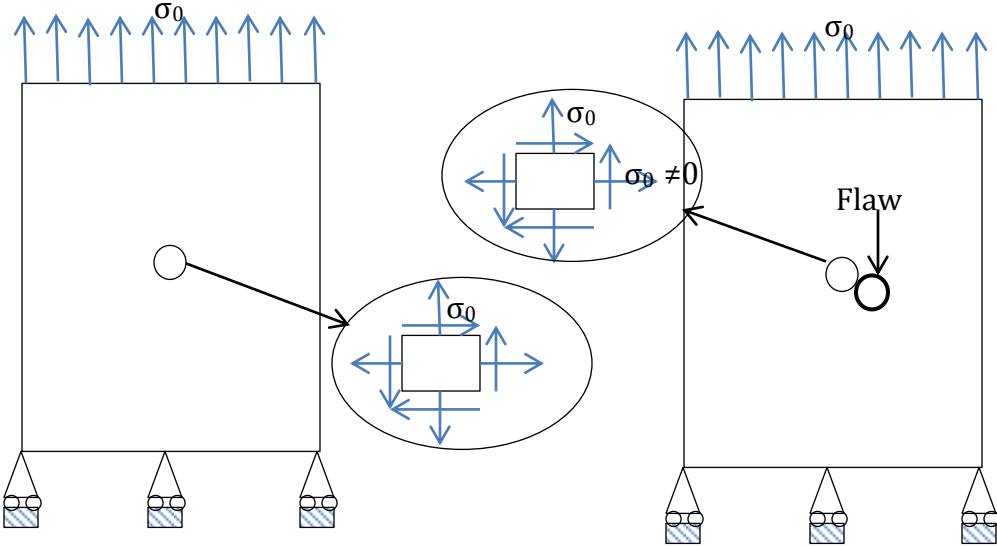**Figure 3.1 A finite tensile plate without and with flaw**

In the first case, the center of flawless plate; the stress field remains equal to the applied stress field σ_0. Therefore the maximum allowable traction can be determined from the condition that the internal stress field should be limited to the material yield stress as a measure of material failure strength.

$$\sigma_0 = \sigma_{yield} \qquad (3.1)$$

In contrast, the elasticity solution for an infinite plate with circular hole or defect predicts the biaxial non-uniform stress field with a stress concentration factor of 3 at the center of the plate, regardless of the size of the hole. In the limiting case of line crack, the solution from a degenerated elliptical hole shown in infinite stress state at a crack tip. No material can withstand such an infinite stress state. Therefore, instead of comparing the existing stress field with strength criterion, fracture mechanics adopts a local stress intensity factor or global energy release rate and compare them with their critical values.

3.2. Modes of fracture failure

State of stress field ahead of the crack tip depends on the curvature of the discontinuity. Usually crack has different curvature. Thus there is a large variation in the stress field near to the crack tip. The curvature of the crack depends upon the modes of the failure and these modes of failure can be divided into three types depending on the loading conditions. Various modes of failure have been shown in Fig. 3.2. Mode I is opening mode and displacement is normal to crack the surface. Mode II is the sliding mode and displacement is in this mode is in plane of the crack. The relative displacement is normal to the crack front. Mode III is also same as Mode II which is caused due to sliding. But in this case displacements are parallel to the crack front, thereby causing tearing.
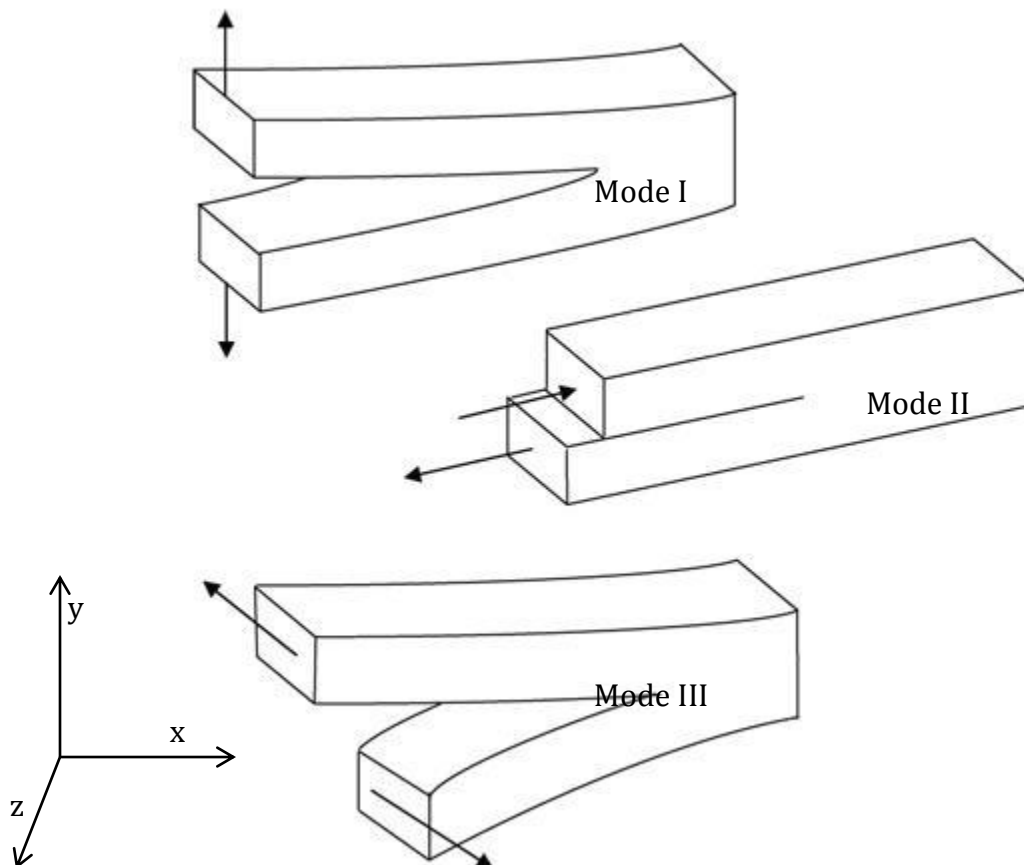

Figure 3.2 Modes of fracture failure

13

An inclined crack can be simulated as the combination of the all the three modes of failure. It can be modeled as superposition of two or three modes of failure depending on the loading criterion. Effect of loading can be analyzed separately for each mode and it can be superimposed under the linear elastic system.

3.3   Stress Intensity Factor

The strength of any material can be defined as the resistance of the body at the extreme loading conditions. This resistance is calculated at the critical part of the domain. In case of fracture problem, the region ahead of the crack tip is very critical. Stress field ahead of crack tip is a function of two variables i.e. loading and the crack length. In the engineering field, solving a problem with two variables is much more difficult. It also impacts on the computational cost. Keeping this point in the mind Irwin (1957) introduced the concept of Stress Intensity Factor (SIF) K, as the measure of strength of the singularity. He illustrated that the entire elastic stress field around the crack tip are distributed similarly and $K \propto \sigma\sqrt{\pi r}$ controls the local stress quantity. Stress field ahead of the crack tip can be expressed as

$$\sigma_{ij} = r^{\frac{-1}{2}}\{K_I f_{ij}^I(\theta) + K_{II} f_{ij}^{II}(\theta) + K_{III} f_{ij}^{III}(\theta)\} + higher\ order\ trems. \qquad (3.2a)$$

Where σ_{ij} is the stress field and K_I K_{II} and K_{III} are the stress intensity factors for the various modes of failure. r and θ are the radial coordinate of the material point. f_{ij}^I is the trigonometric function defined r and θ coordinate system.

$$f_{ij}^I = \frac{1}{\sqrt{2\pi r}}\left(asin\frac{\theta}{2} + bcos\frac{\theta}{2} + csin\frac{3\theta}{2} + dcos\frac{3\theta}{2}\right) \qquad (3.2b)$$

a, b, c, d are the constants. In terms of the applied stress, Stress intensity factor can be expressed as

$$K_I = \lim_{\substack{r\to 0 \\ \theta=0}} \sigma_{yy}\sqrt{\pi r} \qquad (3.3)$$

$$K_{II} = \lim_{\substack{r\to 0 \\ \theta=0}} \sigma_{xy}\sqrt{\pi r} \qquad (3.4)$$

$$K_{III} = \lim_{\substack{r\to 0 \\ \theta=0}} \sigma_{yz}\sqrt{\pi r} \qquad (3.5)$$

Combining the equation (3.2), (3.3), (3.4) and (3.5), we will get the expression for stress field. Stress field and displacement field can be written in terms of stress intensity factor (SIFs). These expressions are as follows:

14

For pure opening Mode I, Stress field is given by

$$\sigma_{xx} = \frac{K_I}{\sqrt{2\pi r}} \cos\frac{\theta}{2} \left(1 - \sin\frac{\theta}{2} \sin\frac{3\theta}{2}\right) \tag{3.6}$$

$$\sigma_{yy} = \frac{K_I}{\sqrt{2\pi r}} \cos\frac{\theta}{2} \left(1 + \sin\frac{\theta}{2} \sin\frac{3\theta}{2}\right) \tag{3.7}$$

$$\sigma_{xy} = \frac{K_I}{\sqrt{2\pi r}} \cos\frac{\theta}{2} \left(\sin\frac{\theta}{2} \cos\frac{3\theta}{2}\right) \tag{3.8}$$

Displacement field is given by,

$$u_x = \frac{K_I}{2\mu} \sqrt{\frac{r}{2\pi}} \cos\frac{\theta}{2} \left(k - 1 + 2\sin^2\frac{\theta}{2}\right) \tag{3.9}$$

$$u_y = \frac{K_I}{2\mu} \sqrt{\frac{r}{2\pi}} \sin\frac{\theta}{2} \left(k + 1 - 2\cos^2\frac{\theta}{2}\right) \tag{3.10}$$

For the pure mode II, Stress field is given by,

$$\sigma_{xx} = \frac{K_{II}}{\sqrt{2\pi r}} \sin\frac{\theta}{2} \left(2 + \cos\frac{\theta}{2} \cos\frac{3\theta}{2}\right) \tag{3.11}$$

$$\sigma_{yy} = \frac{K_{II}}{\sqrt{2\pi r}} \sin\frac{\theta}{2} \left(\cos\frac{\theta}{2} \cos\frac{3\theta}{2}\right) \tag{3.12}$$

$$\sigma_{xy} = \frac{K_{II}}{\sqrt{2\pi r}} \cos\frac{\theta}{2} \left(1 - \sin\frac{\theta}{2} \sin\frac{3\theta}{2}\right) \tag{3.13}$$

Displacement field is given by,

$$u_x = \frac{K_{II}}{\mu} \sqrt{\frac{r}{2\pi}} \sin\frac{\theta}{2}\left(k + 1 + 2\cos^2\frac{\theta}{2}\right) \tag{3.14}$$

$$u_y = \frac{K_{II}}{\mu} \sqrt{\frac{r}{2\pi}} \cos\frac{\theta}{2}\left(k - 1 - 2\sin^2\frac{\theta}{2}\right) \tag{3.15}$$

The tearing mode III has only two non-zero stress components and one non-zero displacement component

$$\sigma_{xz} = \frac{K_{III}}{\sqrt{2\pi r}} \sin\frac{\theta}{2} \tag{3.16}$$

$$\sigma_{yz} = \frac{K_{III}}{\sqrt{2\pi r}} \cos\frac{\theta}{2} \tag{3.17}$$

$$u_x = u_y = 0 \tag{3.18}$$

$$u_z = \frac{K_{III}}{2\mu} \sqrt{\frac{r}{2\pi}} \sin\frac{\theta}{2} \tag{3.19}$$

Where
$$k = \begin{cases} 3 - 4v & Plane\ strain \\ \dfrac{3 - v}{1 + v} & Plane\ Stress \end{cases}$$

v and μ are the Poisson's ratio and bulk modulus respectively.

3.4.   Direct Method to determine the fracture parameters

Finite element analysis of the fracture problem can be done using either triangular element (3 or 6-Noded), or quadrilateral element (4 or 8 Noded). FEM analysis will give the stress and displacement field over the entire domain at the nodal points. Making use of direct available expression of stress and displacement fields [eqns (2.6-2.19)], we can estimate the value of K_I K_{II} and K_{III}.

Ideally K_I and K_{II} should be determined by the stress field at point ahead of the crack tip. It is very difficult to get the stress values ahead of the crack tip. The stress singularities are present at the tip of discontinuity. These stress singularities give a very high SIF value. It is challenging work to mimic the exact stress state ahead of the crack tip. In order to find out the SIF value, we can plot the curve between normalized radius and normalized SIF values for some assumed nodes. This curve will not start from zero

radiuses, hence extrapolation and curve fitting is required for the estimating value at the zero radius. This estimated value can be used as normalized SIF for the given problem.

3.5   Calculation of SIF from J-Integral

J-Integral is defined as

$$J = \int_\Gamma \left(W dx_2 - T_i \frac{\partial u_i}{\partial x_1} ds \right) \tag{3.20}$$

Where $W = \int_0^\varepsilon \sigma_{ij} d\varepsilon_{ij}$ is the strain energy density and T_i is the traction. The contour Γ starts from one crack surface and end at the other end of crack surface as shown in Fig. 3.3. This integral can be evaluated on the path which is slightly away from the crack tip, so that the modeling errors can be minimized. It allows the freedom to make any choice for the computation of the J-Integral. The Path for computation of J-Integral is independent of path.
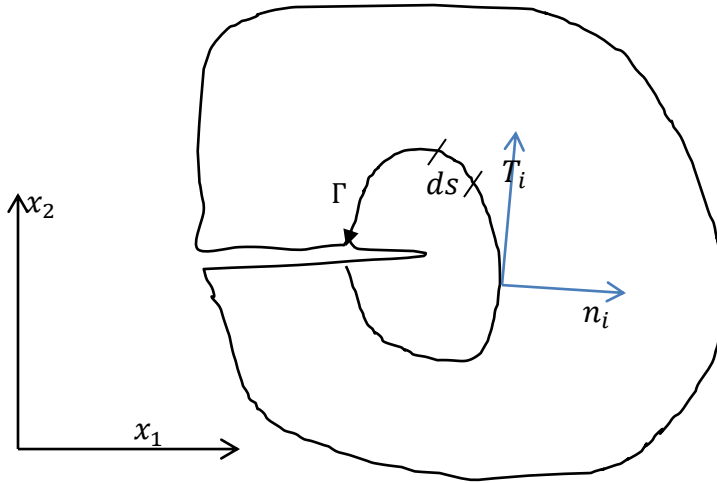
Figure 3.3 Path Γ around the crack tip with outward normal

Knowing the J-Integral value, then the evaluation of the stress intensity factor (SIF) is straight forward. We can use the following expression to calculate the SIFs.

$$J = \frac{K_I^2}{E^*} + \frac{K_{II}^2}{E^*} \tag{3.21}$$

$$\text{Where} \quad E^* = \begin{cases} E & \text{Plane stress} \\ \frac{E}{1-\vartheta^2} & \text{Plane Strain} \end{cases} \tag{3.22}$$

17

3.6 J-Integral: Definition

J – Integral is a characterization parameter of the fracture problem. It characterizes the state of affairs in the region ahead of the crack tip. Energy release density (G) is a special case of the J-Integral. G is limited to the linear elastic material, whereas J-integral is applicable to all kinds of material behavior i.e. linear, non-linear, hyper-elastic and many more. J-integral is best suitable parameter to be determined as the crack tip exhibits the elastic-plastic behavior.

For a plane problem, consider a path Γ around the crack tip which starts from one surface of the crack and ends at the other surface of the crack. This path is arbitrary in nature. It can be smooth or it may have some sharp corner but the path should be continuous and should be within the material. J-integral was first applied to fracture problems for plane problem. J-Integral is defined as

$$J = \int_\Gamma \left(W dx_2 - T_i \frac{\partial u_i}{\partial x_1} ds \right) \tag{3.23}$$

Where $W = \int_0^\varepsilon \sigma_{ij} d\varepsilon_{ij}$ is the strain energy density and T_i is the traction

For 2 –D case W can be expressed in full form as

$$W = \int_0^{\varepsilon_{11}} \sigma_{11} d\varepsilon_{11} + \int_0^{\varepsilon_{12}} \sigma_{12} d\varepsilon_{12} + \int_0^{\varepsilon_{21}} \sigma_{21} d\varepsilon_{21} + \int_0^{\varepsilon_{22}} \sigma_{22} d\varepsilon_{22} \tag{3.24}$$

For symmetric and elastic problem $\sigma_{12} = \sigma_{21}$, hence

$$W = \int_0^{\varepsilon_{11}} \sigma_{11} d\varepsilon_{11} + 2 \int_0^{\varepsilon_{12}} \sigma_{12} d\varepsilon_{12} + \int_0^{\varepsilon_{22}} \sigma_{22} d\varepsilon_{22} \tag{3.25}$$

Traction T_i at the point on the path Γ is expressed through well-known Cauchy's relation $T_i = \sigma_{ij} n_j$. Thus by knowing the stress field and direction of the normal at the point on the path Γ , we can determine the T_i. Finally we can come up with the value of the J-Integral.

3.6.1 Properties of the J-Integral

J-integral has the following properties:

1. J-Integral is path independent, i.e. The path can be any arbitrary path within the domain.
2. For linear elastic materials, the J-integral is same as the energy release rate

3. J-Integral can be related to the crack tip opening displacement δ by the simple relation of the form $J = M\sigma_y \delta$. Where M is dimensionless number, σ_y is far field, δ is opening displacement.

4. J-Integral can be easily determined by the experiments.

3.6.2 Determining the fracture parameter form FEM solution

In general the displacement and stress fields are known as the solution from FEM or any other simulation technique. These displacement fields and stress field can be used to determine the SIF of the problem. SIF can be calculated from the equation given below

$$K_I = \sigma_{ij} \frac{\sqrt{2\pi r}}{g_{ij}^I(\theta)} \tag{3.26a}$$

$$K_I = u_i \frac{\sqrt{2\pi}}{\sqrt{r} f_{ij}^I(\theta)} \tag{3.26b}$$

Where $f_{ij}^I(\theta)$ and $g_{ij}^I(\theta)$ are the functions defined in terms of r and θ [eqn (3.2b)] . σ_{ij} is stress field, u_i is displacement field.

For Mode-I equation 3.26 can be written as

$$K_I = \sigma_{xx} \frac{\sqrt{2\pi r}}{\cos(\frac{\theta}{2})\left(1 - \sin\frac{\theta}{2}\sin\frac{3\theta}{2}\right)} \tag{3.27a}$$

$$K_I = u_i \frac{2(1+v)E\sqrt{2\pi}}{\sqrt{r}\cos(\frac{\theta}{2})\left(1 - 2v + \sin\frac{\theta}{2}\sin\frac{\theta}{2}\right)} \tag{3.27b}$$

Theoretically the crack tip has stress singularity, so to minimize the errors an arbitrary path has been taken for computation of the fracture parameters. SIF has been calculated at all the gauss point along the selected path. This SIF evaluation can be made either from displacement field or from stress field. They are plotted on a graph taking radial distance in x-axis. Both the axes are normalized. Actual SIF value has to be calculated at the crack tip at the radius $r = 0$ but this plotted graph does not give the same. This graph has to be fitted to get the value at zero radius. Curve fitting is done with higher order polynomial to obtain the value at radius zero. This curve fitted value is considered as the SIF. J-Integral is calculated from the equation 3.21.

19

Chapter 4

Generalized finite element Method

4.1 Introduction

In order to model the discontinuous displacement field, a special shape functions are required to capture the approximate behavior. These special shape functions are enriched with the help of some additional enrichment functions and associated shape functions are called enriched shape function. The method operates on the additional independent virtual degree of freedom for the definition of crack boundary and the approximation of the displacement field.

4.2 Realization of enrichment function in 1-D

To understand the behavior of the additional enrichment function, we have demonstrated the various kinds of enrichment function. We have plotted the variation of shape functions with the effects of enrichment functions. To illustrate and validate the above statement, we have taken a 1-D problem Fig.4.1 (a). The domain has been discretized into 4 elements as shown in Fig.4.1 (b). Variation of classical FEM shape function has been illustrated in the Fig. 4.1 (c).
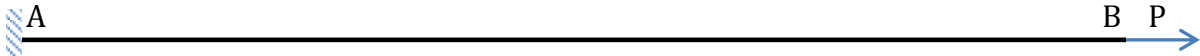
Figure 4. 1 (a) Domain
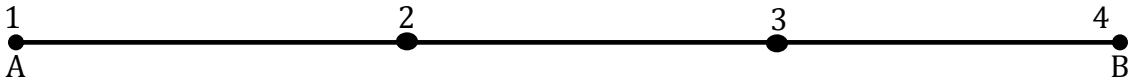
Figure 4.1 (b)   Discretize Domain using 2 noded 1D element
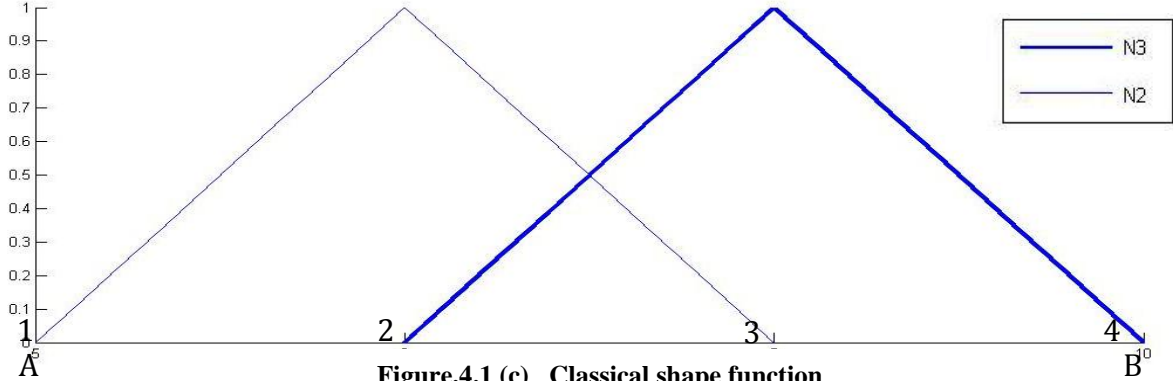
Figure.4.1 (c)   Classical shape function

If the same domain has a discontinuity as shown in Fig.4. 2 (a) as well as the discretization is also same as for the continuous domain, then Node 2, 3 are required to be enriched, whereas Node 1 & 4 are not influenced by the discontinuity.
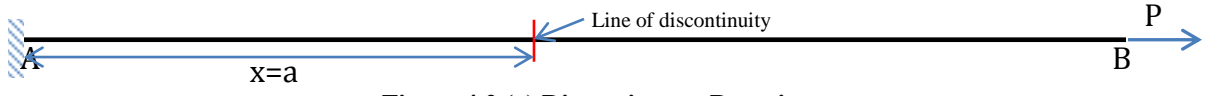
Figure.4.2 (a) Discontinuous Domain
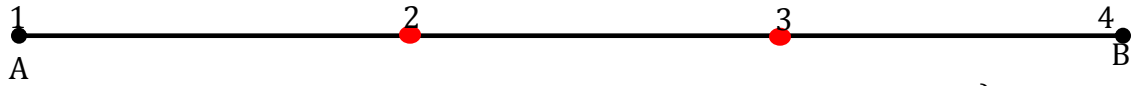
Figure.4.2 (b) Discretize Domain (Red Point –Enriched Node)

There have been a number of possibilities of enrichment function, which can be used to simulate the strong discontinuity in the domain. Few of them are illustrated here.

Enrichment function in 1-D

4.2.1 Partition of Unity Method: A simple Model

In the development stage of XFEM, many researchers had used the concept of partition of unity approach to find out the enriched shape functions. Enriched shape function has been defined as the following

$$\varphi_i^h = \begin{cases} \varphi_i - 1 & x \in \Omega_i \\ \varphi_i & x\Omega_i \end{cases} \qquad (4.1)$$
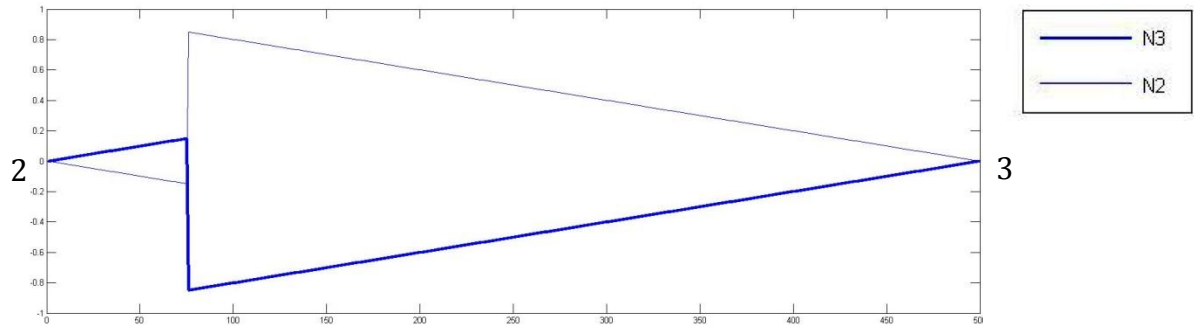
Figure 4.3 Jumps in the shape function using the Partition of Unity Concept

Fig. 4.3 shows the jump in the basis functions which are capable of capturing the discontinuity in the domain. This kind of jump function provides the same strain field in the both sides of the discontinuity. This is in contrast to independent physical response of segment anticipated in

21

cracked domain. For this jump methodology, a lesser number of additional Dofs are required than other methods. Thus it cannot be a better method to be used for simulating the cracked domain.

4.2.2 The Heaviside function

Heaviside function has been defined in various manners over a decade. Definition of Heaviside function has been modified depending on the problem statement. Classical or first type of Heaviside function has been defined on the basis of step function. Mathematically it can be written as an equation (3.2). A variation of it has been shown in Fig. 4.4 (a).

$$H(x) = \left\{ \begin{array}{ll} 1 & \forall x > 0 \\ 0 & \forall x < 0 \end{array} \right. \tag{4.2}$$
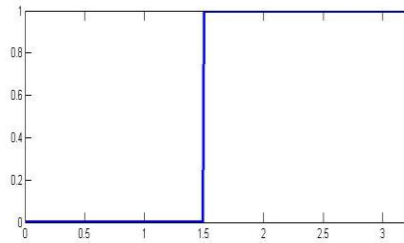
Figure.4.4 (a) Step Heaviside Function

The effect of the step Heaviside function has been shown in Fig. 4.4 (b). Now the strain fields are independent for the both sides of the discontinuity. Here shifting is defined as the difference between the classical and enriched shape function and it has been shown in Fig.4.4 (c). If we see the variation of the shape function, it has value equal to the zero on the left side of discontinuity. This observation shows that these types of enrichment functions are not capable of capturing the exact behavior in the both sides of cracked domain.
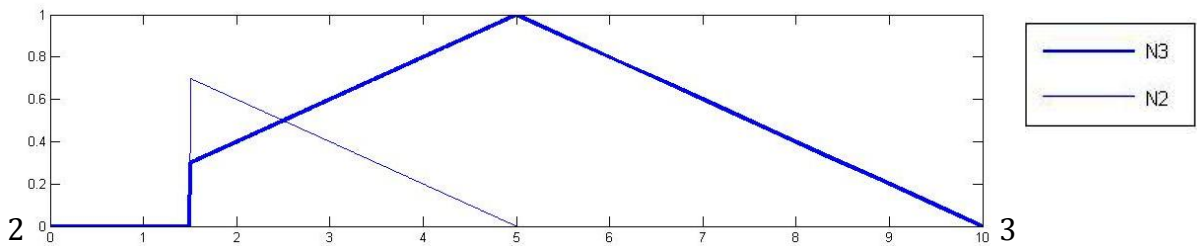
Figure 4.4 (b) Effect of Step Heaviside Function on 1-D FEM Shape function

2   3
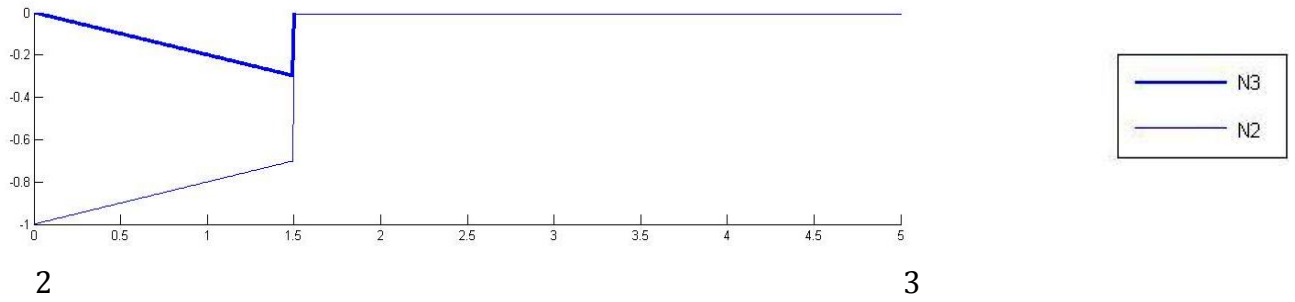
Figure 4.4 (c) Shifting of 1-D FEM shape function

4.2.3   Modified Heaviside function

To increase the capability of Heaviside function, it has been modified with the help of the sign function. It is also called as signed Heaviside function. It can be expressed as follows

$$H(x) = \left\{ \begin{array}{ll} 1 & \forall x > 0 \\ -1 & \forall x < 0 \end{array} \right. \tag{4.3}$$

The variation of the modified Heaviside function is shown in Fig.4.5 (a). It has value equal to 1 and -1, which helps in capturing the behavior in the both sides of the crack. It also ensures the independency of the strain field in the both sides of the discontinuity. Enriched shape function variation has been plotted in the Fig.4.5 (b) and its shifting has been illustrated in Fig. 4.5 (c).
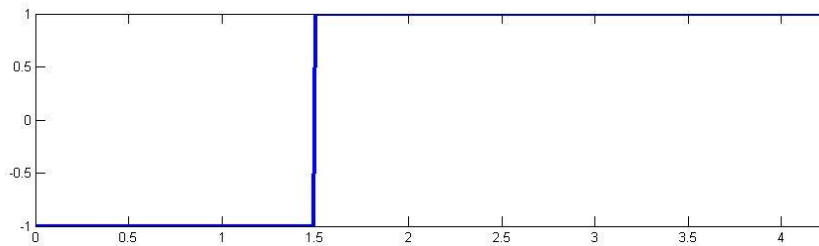
Figure 4.5 (a)   Sign Heaviside Function

2   3
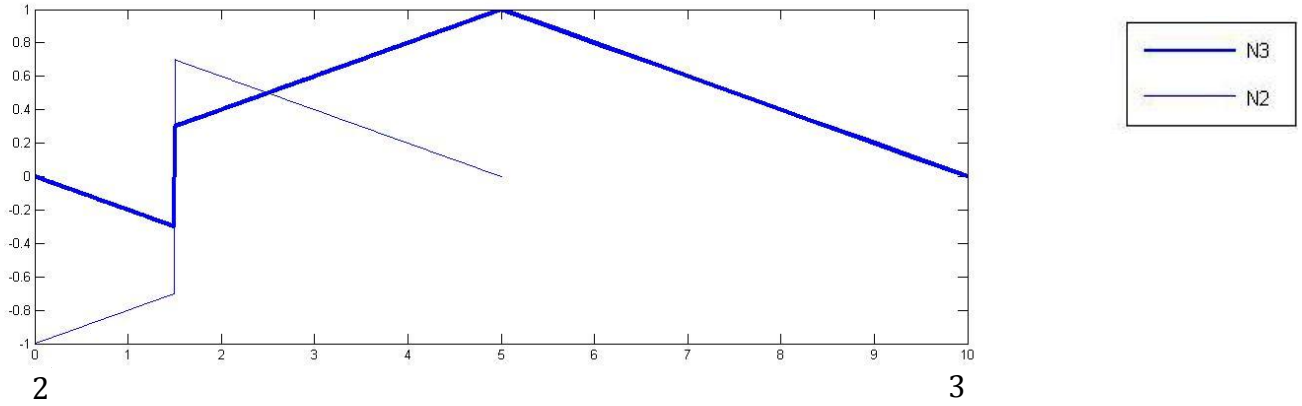
Figure 4.5 (b)   Effect of Sign Heaviside Function on 1-D FEM shape function

2   3
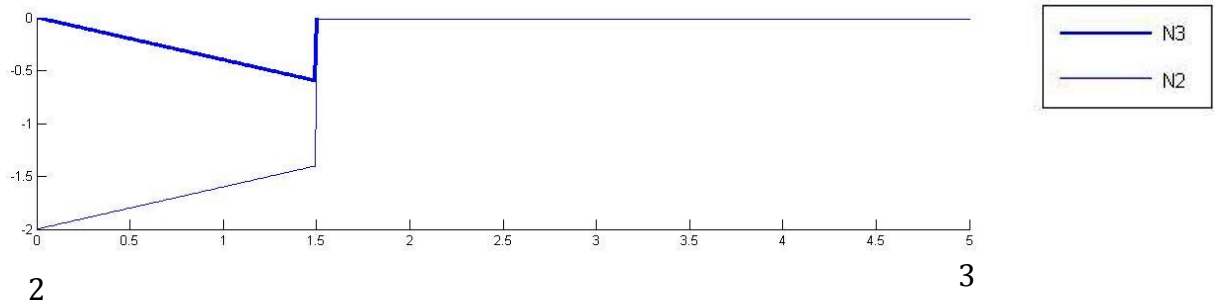
Figure 4.5 (c) Shifting of 1-D FEM shape function

4.3 Realization of enrichment function in 2-D

The main objective of enrichment function is to reproduce the singularity around the crack tip. It can be achieved by using terms containing trigonometric functions. In order to model the discontinuous displacement field, a special kind of shape functions is required to capture the approximate behavior. The method operates on the additional independent virtual degree of freedom for the definition of crack boundary and the approximation of the displacement field.
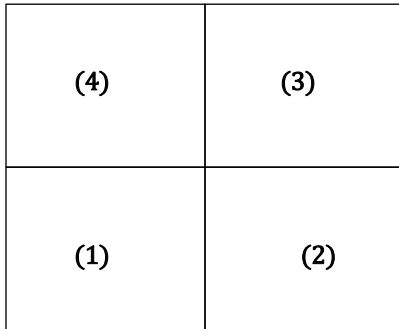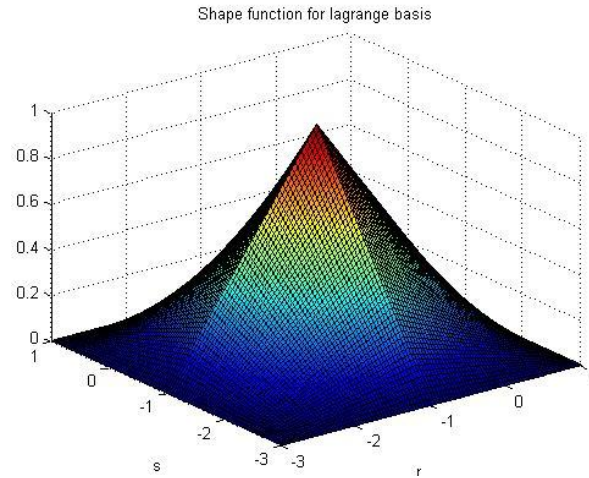
Figure 4.6 (a) Patch of 4-element (b) Classical shape function or hat function

Various kinds of enrichment function for 2 –D are listed below

- Modified Heaviside function
- Crack tip enrichment function
- Level set enrichment function

The variation and its effect on the approximation function have been discussed in the following section.

4.3.1 Modified Heaviside function

Heaviside function is discontinuous along the crack path which insures the presence of discontinuity in the approximation. These discontinuities can be easily modeled using these kinds of enrichment function. A variation of the Heaviside function is shown in the Fig 4.7. Mathematically it can be written as follows:

$$H(\xi) = \begin{cases} 1 & \forall \xi > 0 \\ 0 & \forall\, \xi = 0 \\ -1 & \forall\, \xi \leq 0 \end{cases} \tag{4.4}$$

25
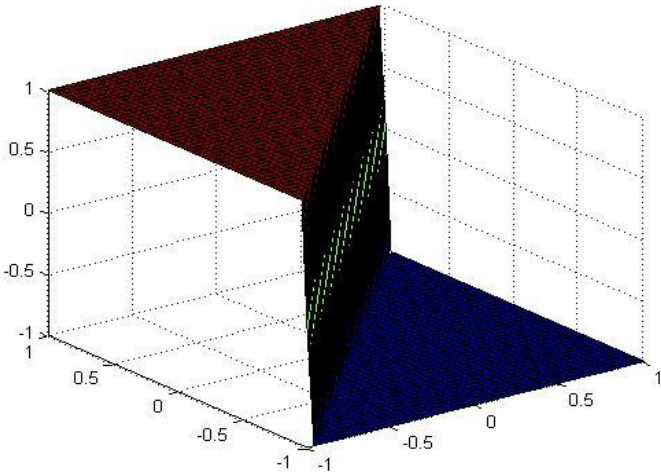
(a)
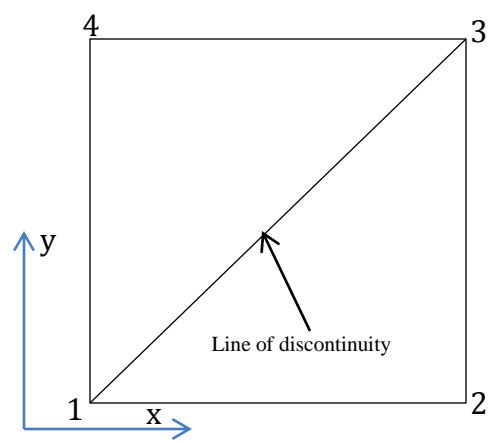
(b) Bilinear element

Figure 4.7 (a) Variation of Modified Heaviside Enrichment function in 2-D   (b) Cracked Domain
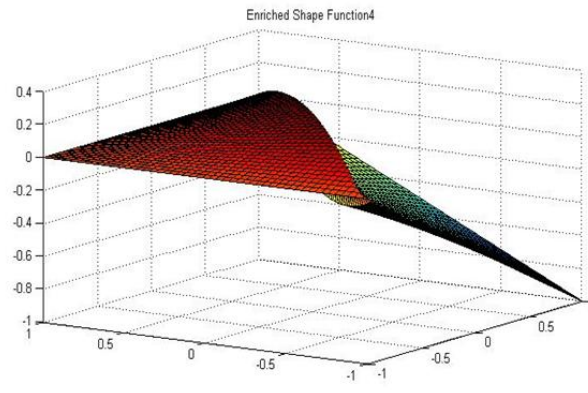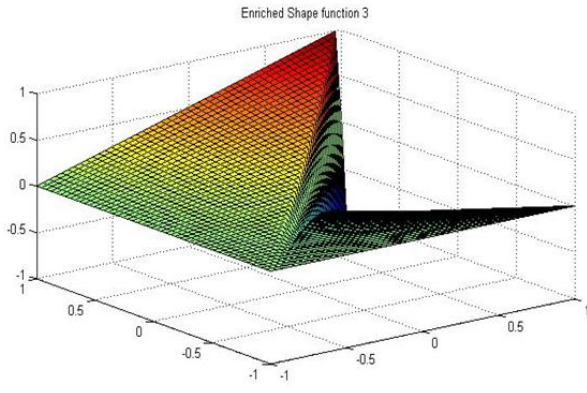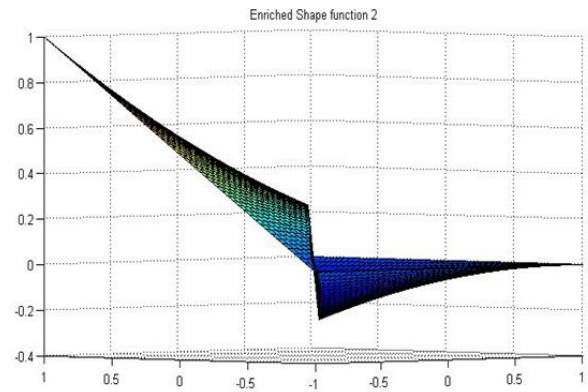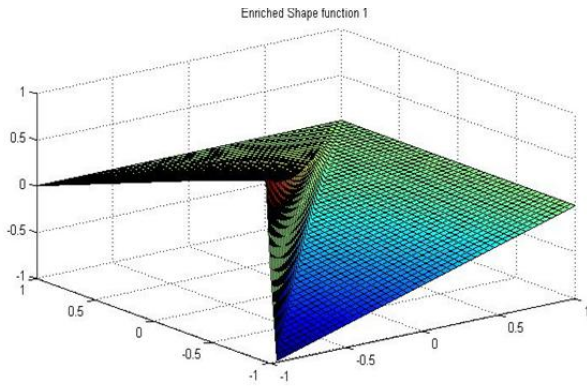
Figure 4.8 Variation of enriched shape function (N_1-N_4) with implementation of Modified Heaviside Enrichment

If an element has a crack as shown in the Fig.4.7 (b), then the variation of Heaviside function is as shown in Fig. 4.7 (a). When this enrichment function is multiplied with the classical shape function or hat function, then enriched shape functions are obtained. These enriched shape functions are depicted in the Fig. 4.8.

4.3.2   Crack tip Enrichment function

The near tip enrichment is defined in terms of local crack tip coordinate system (r, θ). $\emptyset_i = \left\{ \sqrt{r} \sin\left(\frac{\theta}{2}\right),\ \sqrt{r} \cos\left(\frac{\theta}{2}\right),\ \sqrt{r} \sin\left(\frac{\theta}{2}\right) \sin(\theta),\ \sqrt{r} \cos\left(\frac{\theta}{2}\right) \sin(\theta) \right\}$. The main objective of enrichment function is to reproduce the singularity around the crack tip. It can be achieved by using terms containing trigonometric functions. The tip enrichment function contains the sine and cosine function, which ensures the presence of crack inside the element. The square root of radial distance has ability to reproduce the singularity at the crack tip. Remember that radial distance has been defined with respect to the crack tip point. The angle for trigonometric functions should lie in between pi to (–pi). The variation of these enrichment functions is shown in the Fig. 3.9 and its effect can be easily visualized in the Fig. 4.10.
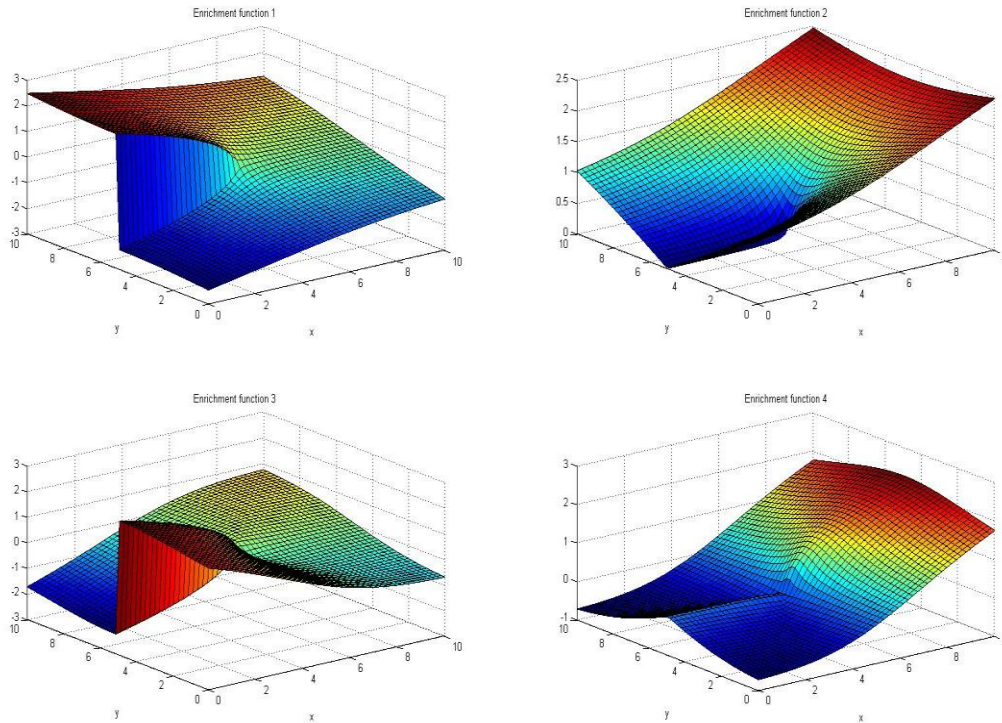
Figure 4.9 Crack-tip Enrichment function
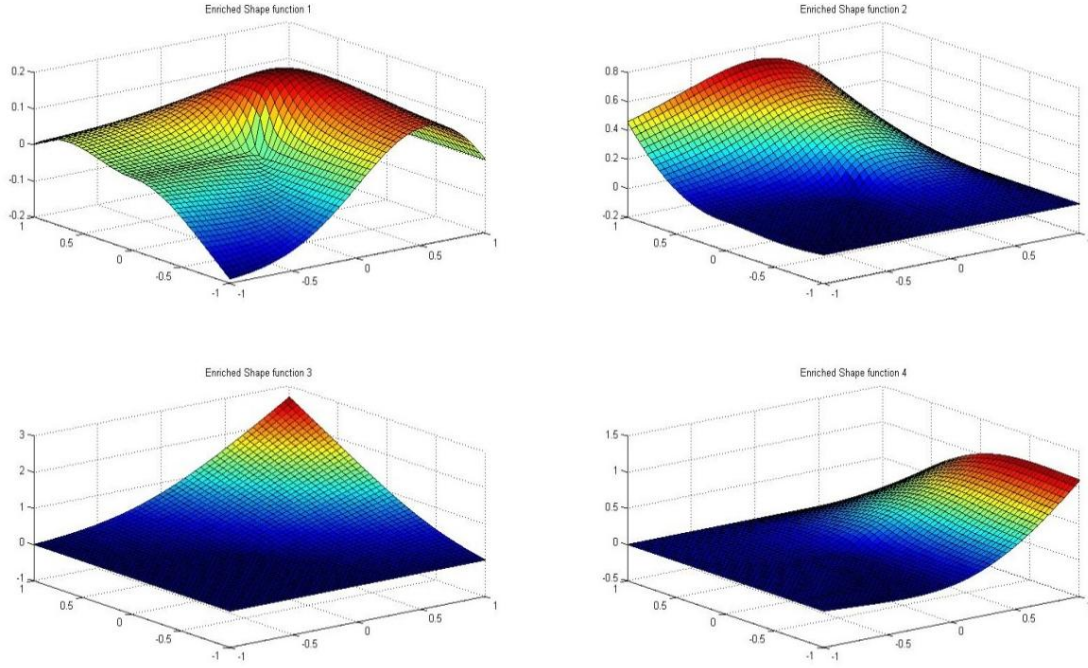
Figure 4.10 Basis function with Crack-tip Enrichment function

4.3.3 Enrichment function by Level set

The level set function is defined as a function of location of crack propagation. And the minimum distance has been plotted a surface plot in Fig 4.11. This has been used as enrichment function. These enrichment functions are most suitable for dislocation and hole modeling problems. The effects of these enrichment functions can be seen in Fig 4.14. Mathematically level set can be expressed as follows.

$$\emptyset(x) = \begin{cases} d(x) & \forall \, x \in \Omega^+ \\ 0 & \forall \, x \in \Gamma \\ -d(x) & \forall \, x \in \Omega^- \end{cases} \qquad (4.5)$$

$$d(x) = \min \; \|x_r - x_\Gamma\| \qquad (4.6)$$

28
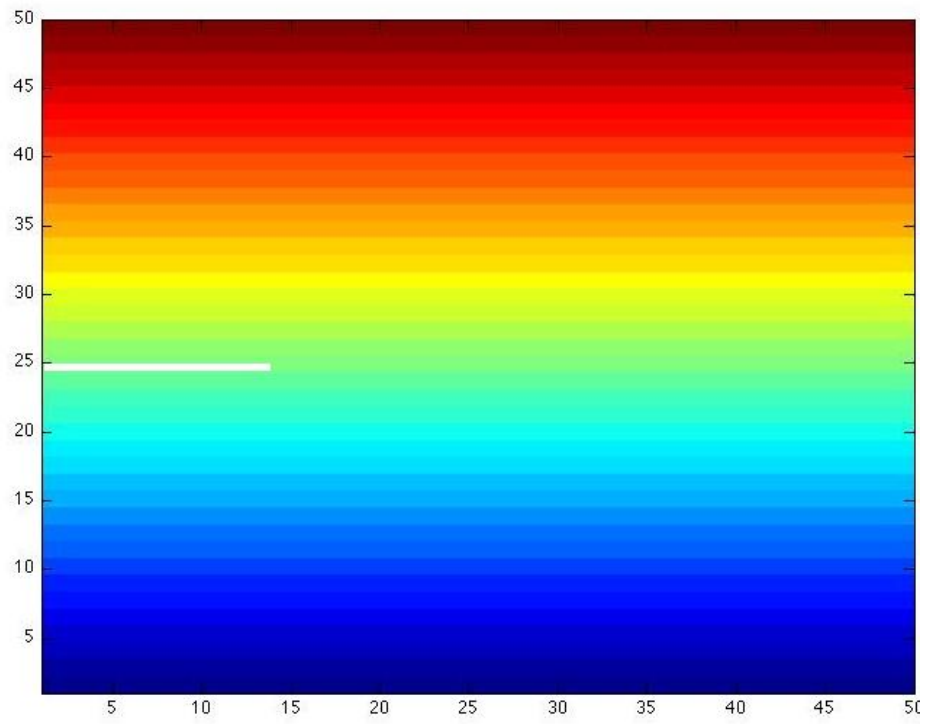
Figure 4.11 Level set in Y-direction
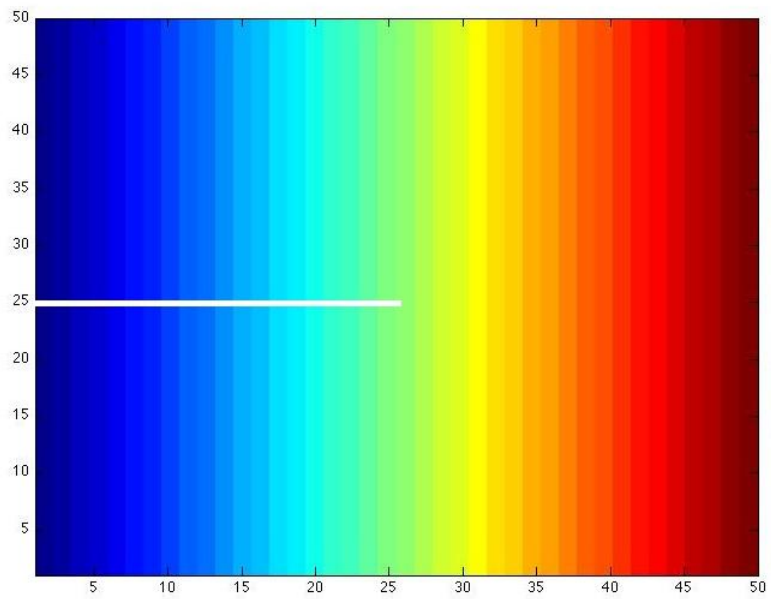
Figure 4.12 Variation of the level set function in X-direction
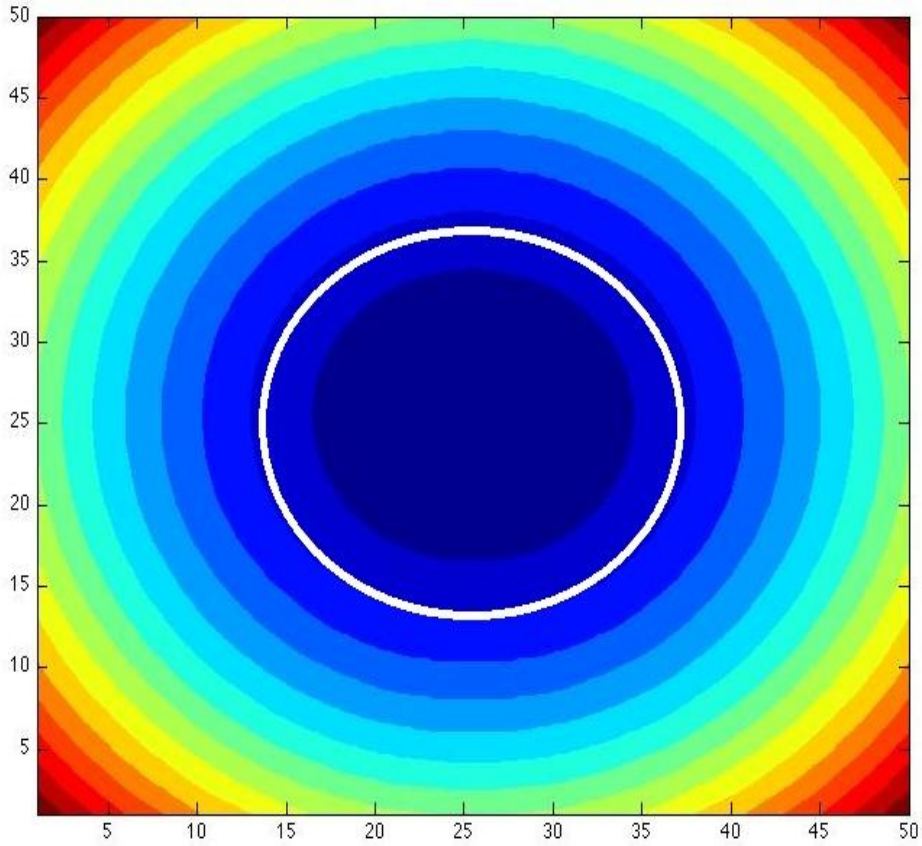
Figure 4.13 Variation of Level set function in case of inclusion or circular discontinuity

Fig. 3.11 illustrates the variation of a minimum distance of the point from the cracked portion. Mathematically it is the perpendicular distance between the point and the crack. Fig 3.12 shows the variation in the Y-direction. It is the minimum distance between the crack tip and any arbitrary point in the domain. In case of inclusion and circular discontinuities, level set is defined on the basis of radial distance of the material point. It depends on the given radius of inclusion. The variation of such kind of level set is presented in the Fig. 3.13. These level set functions are very good in capturing the dynamic crack. Level set function for arbitrary crack has been plotted in the Fig. 3.14. Enriched shape function is also plotted in the same figure.
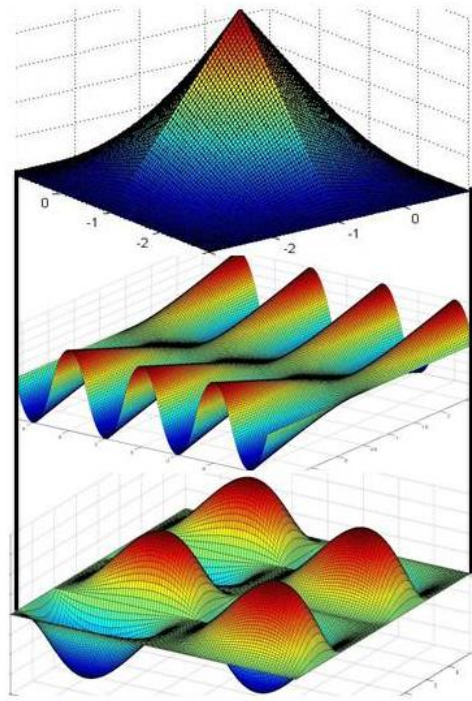
Figure 4.14 Top: hat function or classical shape function, Middle: Level set to arbitrary crack, Bottom: Enriched shape function with the implementation of middle function. Enriched shape function is obtained by the multiplication of the hat function and level set

4.4 Conclusion

Enrichment functions are the key function in GFEM context. These enrichment functions are capable to mimic the exact behavior ahead of the crack tip. Level set based enrichment functions are capable to entertain the material behavior in the simulation of composite materials. 3-D crack can be captured with the help of the level set based enrichment functions. The various enrichment functions have been studied in this chapter. Their application and their potential have been described through examples. 1-D and 2-D examples have been illustrated here.

Chapter 5

Blending Element

5.1 Introduction

Application of the enrichment near the crack tip analysis leads to solution incompatibility and interior discontinuities, if it is not employed in the entire domain. Since neighboring domains are using the different basis function and approximation, it can attribute the incompatibility of the solution. There is a transition from classical FEM approximation to the enriched FEM approximation. As a result the different value may be obtained for the same node. Occurrence of the different values shows the interior discontinuities.

Main Issue related transition of approximation in GFEM

1. Convergence of the solution is not guarantied.
2. Enrichment does not follow the partition of unity method properties. Hence the order of convergence and error may get affected

Seeing these drawbacks in GFEM/X-FEM, It became an essential requirement to rewrite the approximation for Blending elements. It is suggested to write down the approximation in the following form

$$u^h(x) = \sum_{i \in I} N_i(x)\, u_i + R(x) \sum_{\alpha} \sum_{j \in I} N_j(x)\varphi_\alpha(x)a_{j\alpha}$$

Where $R(x)$ is called Ramp function or Blending functions, $N_i(x)$ are classical shape function, φ_α enriched shape functions, $a_{j\alpha}$ are the additional Dofs . All other terms have usual meaning. This function should have some essential properties.

5.2 Problem Statement

1. A blending function, which can be helpful in a smooth transition between enriched, and unenriched domain (Classical domain) is required.

32

2. Enrichment function, which should not produce parasite, terms in the approximation so that the ability to reproduce the stress/strain condition can be retained.

5.3 Literature Survey

Blending element was first introduced by Sukumar [52] in XFEM with the level set method. In this work they had used ramp function as blending function. Blending element is an element whose some of the nodes are enriched and some of the nodes are classical node. A broad framework has been developed by Chessla et.al [28, 29, 32] to sort out the problems associated with parasitic terms in the approximation. To this end enrichment of the strain field is done instead of directly enriching the approximation.

Many researchers have used so many techniques to sort out the problems related to blending elements. Chessla et.al [32] had used assumed strain method to eliminate the parasite terms in the approximation. The larger approximation space of higher order spectral element has been also shown to improve the accuracy in the blending element. Gracie [53] has used discontinuous Galerkin [54] method to overcome the spurious behavior of blending element. In this method domain is divided in two parts as enriched and unenriched patches, which are independently discretized. Continuity in the patches is enforced in the weak sense by internal penalty method. Intrinsic XFEM and discontinuous enrichment methods are two methods to not have blending elements. Fries [55] have proposed a method based on the weighting of enrichment that vanishes at the edge of enriched subdomain.

5.4 Classification of the elements

Due to different approximation function, finite elements used in GFEM can be classified into three categories

(a) Classical Element
(b) Enriched Element
(c) Blending Enrichment or Partial Enriched Element

First two categories are fully governed by the classical and enriched approximation respectively, whereas the blending element is governed by the combination of both approximations. Classification of the element is shown in the Fig. 5.1. In the Fig. 5.1 green color shows the element with discontinuity, which has enriched approximation. The neighboring elements shown in red color are partially enriched element. They are governed by the combination of approximation of classical as well as enriched approximation. Remaining blue color elements are the classical elements, which are governed by the classical approximation.
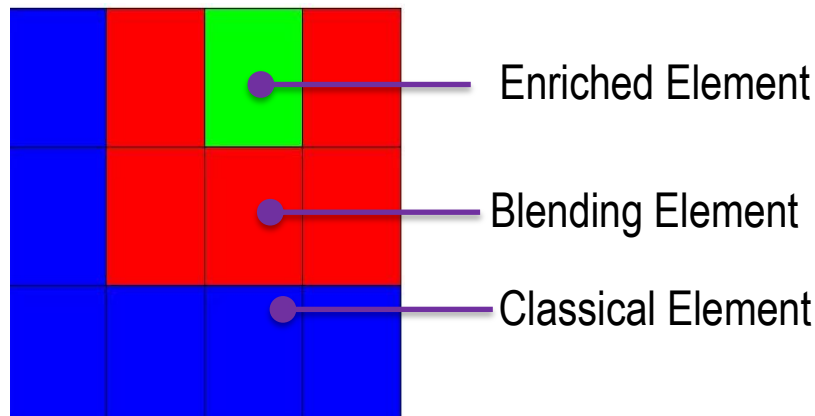
Figure 5.1 Classification of Element a) Green- Enriched (b) Red- Blending (c) Blue- Classical Element

5.5 Characteristics of Blending or Ramp function

Linear and spline function are frequently used as ramp function. These functions should have the following characteristics in them.

1. Define the appropriate ramp function to satisfy the C^0 and C^1 continuity between the enrichment and classical finite element approximation.
2. Linear and spline functions are usually preferred.
3. The size of transition zone should be selected.
4. Compute the necessary term associated with the transition domain.
5. The number of enriched and classical nodes in the transitional finite element may suddenly change in nearby elements. Special precautions are required to avoid potential mistakes in defining the correct numbers for different summation.

5.6 Properties of Blending Function:

1. **Co-ordinate independent:** Blending functions should be co-ordinate independent. It emphasizes that the function should not change in as there is any change in coordinate system. In order to show for co-ordinate independency blending function should follow the Partition of Unity (POU). The property of co-ordinate independence is also called as affine invariance. Mathematically id can be written as

$$\sum_{i=1}^{n} R_1 = 1$$

2. **Convex hull properties**: Convex hull is set of point in X in a real vector space which contains the optimal and minimal points. This property exists in the functions which are co-ordinate independent. In this case the blending function is non-zeros. Mathematically it can be expressed as follows:

$$\sum_{i=1}^{n} R_i(t) \equiv 1, \quad R_i(t) \geq 0, \quad 0 \leq t \leq 1$$

3. **Symmetric functions**: if the function value does not change with the change of sequence of data points or domain, then these functions are called as symmetric function. For a function symmetricity can be assured if and only if

$$\sum_{i=1}^{n} R_i(t)P_i \equiv \sum_{i=1}^{n} R_i(1-t)P_{n-i} \qquad 0 < t < 1$$

This hold true if $R_i(t) = R_{n-i}(1-t)$

4. **Variation Diminishing Properties**: B-Spline and Bezier always obey these properties. It says that if a given straight line intersects the curve in c number of points and the control polygon in p numbers of point then it will hold true

$$c = p - 2j$$

Where j is any positive integer

5. **Linear Independence**: A set of blending functions is linearly independent. Mathematically it can be written as follows

$$\sum_{i=1}^{n} a_i R_i \equiv 0$$

Where a_i are random constants. If blending functions are not linear independent, then one function can be written as a combination of other functions. This will affect the order of approximation.

6. **End Point interpolation**: Blending functions are interpolatory in nature. But they interpolate the value at the end points. Due to this interpolation properties blending function are much more useful in X-FEM/G-FEM. It interpolates the value of classical node as well as at enriched node. This provides a smooth transfer from classical to enriched approximation.

5.7 Examples of Blending Function:

a. **1st order Blending Function:** It has value as zero or one. It's defined as the following

$$R_1(t) = \begin{cases} 1 & 0 \leq t \leq 1 \\ 0 & otherwise \end{cases}$$

b. **2nd order Blending Function:** it's obtained from the 1st order blending function. After integrating the 1st order blending function, 2nd order is obtained. It is defined as the following

$$R_2(t) = \int R_1(t)dt$$

35

$$R_2(t) \equiv \begin{cases} t & 0 \le t \le 1 \\ 2 - t & 1 \le t \le 2 \end{cases}$$

c. **3rd order Blending Function:** 3rd order is obtained from the integration of 2nd order blending function. It has been defined as the follows

$$R_3(t) = \int R_2(t)dt$$

$$R_3(t) \equiv \begin{cases} \dfrac{1}{2}t^2 & 0 \le t \le 1 \\ \dfrac{1}{2}(-2t^2 + 6t - 3 & 1 \le t \le 2 \end{cases}$$

(a)

(b)

(c)

$R(x)$
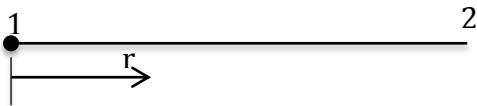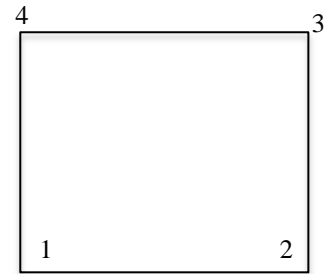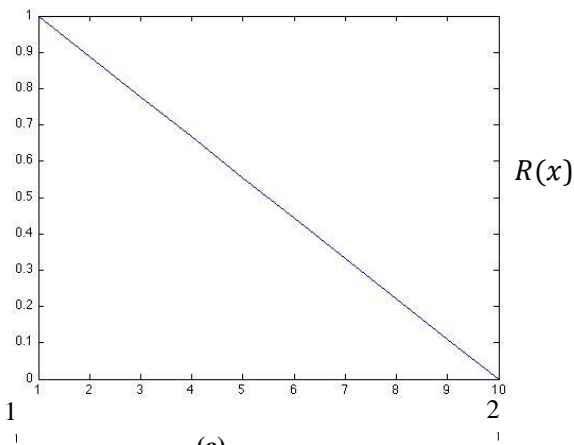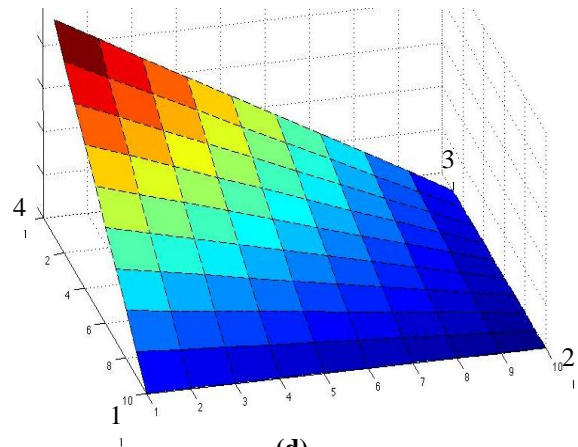
(d)

Figure 5.2 (a) 1D blending element (b) bilinear blending element, Variation of Blending or Ramp function in (c) 1D (d)2D

5.8 Blending Function used in Thesis

Our approach is based on local enrichment function, which results out as transition of approximation between the two neighboring elements. Thus the blending element became an important issue. As we have seen earlier that it can be solved using the blending function. There are various kinds of Blending functions. We have used first order Blending function as shown in Fig.5.2.

Blending function has variation from 0 to 1. It has value equal to one of the enriched node and has a value equal to zero at all other nodes. Fig. 5.2 (a) and (b) shows the 1-D and 2-D domain respectively. Lets assume that node 1 is enriched incase of 1-D and node 4 in case of 2-D problem (Fig.5.2 (a) & (b). All other nodes are classical nodes. For one dimensional and 2-dimensional problem, variations are shown in the Fig.5.2 (c) and (d) respectively.

The strategy follows the following steps:

(a) Begins with standard partition of unity approximation
(b) Multiply the origin enrichment function by monotonically decreasing weight function with compact support.
(c) Constrained all the enriched degree of freedom to be equal. Weight function is used in such a manner to avoid inter-element discontinuity.

5.9 Conclusion

In this chapter various blending functions has been studied. This chapter emphasis on the need of the blending functions. Classification and properties of the blending functions are described in detail. Variation of the blending function has been demonstrated though an example. Implementation strategy has been discussed.

.

Chapter 6

Galerkin Formulation and GFEM Implementation

6.1 Introduction

This chapter is concerned with Galerkin formulation of equilibrium governing equation. Classical formulation is limited to classical degree of freedom but in case of GFEM some additional degree of freedoms are introduced. These additional degrees of freedoms are consolidated to the discontinuous element. The formulation of these discontinuous elements allows the simulation of the crack propagation without remeshing. A detail of the numerical implementation has been given in this chapter.

6.1.1 Governing Equation

Consider a body in the state of equilibrium with the boundary conditions in the form of tractions and displacement conditions as shown in the Fig.6.1
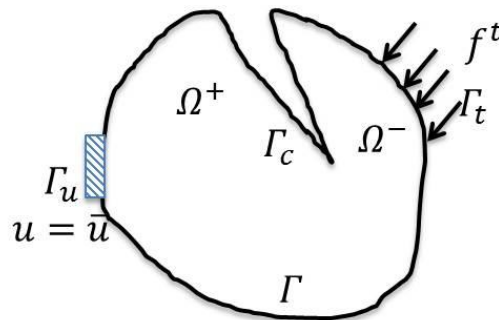
Figure 6.1 Body in static equilibrium

The strong form of the equilibrium equation can be written as

$$\nabla.\sigma + f^b = 0 \quad in \quad \Omega \qquad (6.1)$$

With the Boundary conditions

$$\begin{cases} \sigma.n = f^t & on\ \Gamma_t \\ u = \bar{u} & on\ \Gamma_u \\ \sigma.n = 0 & on\ \Gamma_c \end{cases} \qquad (6.2)$$

Where Γ_t, Γ_u, and Γ_c are the traction, displacement, and cracked boundaries respectively. σ is the stress 1st order tensor. f^b is the body force. f^t is the applied traction force on the traction boundary.

From the principle of virtual work, the variational formulation of the boundary value problem can be defined as

$$W^{int} = W^{ext} \qquad (6.3)$$

Integral form of the equation can be written as

$$\int \sigma.\delta\varepsilon\,d\Omega = \int f^b \delta u\,d\Omega + \int f^t.\delta u\,d\Gamma \qquad (6.4)$$

5.1.2 GFEM discretization

The discretization of the equation (6.4) using the GFEM approximation (equation (6.1)) results into the system of linear equilibrium equations:

$$Ku^h = f \qquad (6.5)$$

Where K is the stiffness matrix. u^h is the vector of nodal freedom (enriched and classical combined), f is the vector of the external forces. The global matrix and vectors are calculated by the assembling the element stiffness matrix and element vectors. K and f for each element e are defined as

$$K_{ij}^e = \begin{bmatrix} K_{ij}^{uu} & K_{ij}^{ua} & K_{ij}^{ub} \\ K_{ij}^{au} & K_{ij}^{aa} & K_{ij}^{ab} \\ K_{ij}^{bu} & K_{ij}^{ba} & K_{ij}^{bb} \end{bmatrix} \qquad (6.6)$$

$$f_i^e = \{f_i^u\ f_i^a\ f_i^{b1}\ f_i^{b2}\ f_i^{b3}\ f_i^{b4}\} \qquad (6.7)$$

And u^h is the vector of nodal parameters

$$u^h = \{u\ a\ b_1\ b_2\ b_3\ b_4\} \qquad (6.8)$$

With

$$K^{rs} = \int (B^r)^T D B^s d\Omega \qquad (r, s = u, a, b) \qquad (6.9)$$

$$f_i^u = \int_{\Gamma_t} N_i f^t d\Gamma + \int_{\Omega} N_i f^b d\Omega \qquad (6.10)$$

$$f_i^a = \int_{\Gamma_t} N_i H f^t d\Gamma + \int_{\Omega} N_i H f^b d\Omega \qquad (6.11)$$

$$f_i^{bk} = \int_{\Gamma_t} N_i \emptyset_k f^t d\Gamma + \int_{\Omega} N_i \emptyset_k f^b d\Omega \quad (k = 1,2,3,4) \qquad (6.12)$$

In the equation (6.9) , the B is the shape function derivative.

$$B_i^u = \begin{bmatrix} N_{i,x} & 0 \\ 0 & N_{i,y} \\ N_{i,y} & N_{i,x} \end{bmatrix} \qquad (6.13)$$

$$B_i^a = \begin{bmatrix} (N_i H)_{,x} & 0 \\ 0 & (N_i H)_{,y} \\ (N_i H)_{,y} & (N_i H)_{,x} \end{bmatrix} \qquad (6.14)$$

$$B_i^b = \begin{bmatrix} B_i^{b1} & B_i^{b2} & B_i^{b3} & B_i^{b4} \end{bmatrix} \qquad (6.15)$$

$$B_i^k = \begin{bmatrix} (N_i \emptyset_k)_{,x} & 0 \\ 0 & (N_i \emptyset_k)_{,y} \\ (N_i \emptyset_k)_{,y} & (N_i \emptyset_k)_{,x} \end{bmatrix} \qquad (6.16)$$

Where $k = 1,2,3,4$.

The crack tip enrichment functions have been defined in the terms of the local crack tip co-ordinate system (r, θ) as shown in the Fig.6.2. Mathematically it can be rewritten as

$$\emptyset_k(r, \theta) = \left\{ \sqrt{r} sin\frac{\theta}{2}, \sqrt{r} cos\frac{\theta}{2}, \sqrt{r} sin\theta sin\frac{\theta}{2}, \sqrt{r} sin\theta cos\frac{\theta}{2} \right\} \qquad (6.17)$$

Derivative of $\emptyset_k(r, \theta)$ with respect to the crack tip polar coordinate becomes

$$\emptyset_{1,r} = \frac{1}{2\sqrt{r}} sin\frac{\theta}{2} \qquad (6.18)$$

$$\emptyset_{1,\theta} = \frac{\sqrt{r}}{2} cos\frac{\theta}{2} \qquad (6.19)$$

$$\emptyset_{2,r} = \frac{1}{2\sqrt{r}} cos\frac{\theta}{2} \qquad (6.20)$$

$$\emptyset_{1,\theta} = \frac{\sqrt{r}}{2} sin\frac{\theta}{2} \qquad (6.21)$$

$$\emptyset_{3,r} = \frac{1}{2\sqrt{r}}\sin\theta\sin\frac{\theta}{2} \tag{6.22}$$

$$\emptyset_{3,\theta} = \sqrt{r}\left(\frac{1}{2}\cos\frac{\theta}{2}\sin\theta + \sin\frac{\theta}{2}\cos\theta\right) \tag{6.23}$$

$$\emptyset_{4,r} = \frac{1}{2\sqrt{r}}\sin\theta\cos\frac{\theta}{2} \tag{6.24}$$

$$\emptyset_{4,\theta} = \sqrt{r}\left(-\frac{1}{2}\sin\frac{\theta}{2}\sin\theta + \cos\frac{\theta}{2}\cos\theta\right) \tag{6.25}$$

Where r and θ are defined in terms of the global coordinate systems

$$r_i = \sqrt{\left(x_i - x_{tip}\right)^2 + \left(y_i - y_{tip}\right)^2} \tag{6.26}$$

$$\theta_i = \tan^{-1}\left(\frac{y_i - y_{tip}}{x_i - x_{tip}}\right) \tag{6.27}$$

The derivative of the r and θ with respect to the global coordinate system can be written as

$$r_{i,x} = \frac{1}{2}\frac{2(x_i - x_{tip})}{\sqrt{\left(x_i - x_{tip}\right)^2 + \left(y_i - y_{tip}\right)^2}} \tag{6.29}$$

$$r_{i,y} = \frac{1}{2}\frac{2(y_i - y_{tip})}{\sqrt{\left(x_i - x_{tip}\right)^2 + \left(y_i - y_{tip}\right)^2}} \tag{6.30}$$

$$\theta_{i,x} = \frac{1}{1 + \left(\frac{y_i - y_{tip}}{x_i - x_{tip}}\right)^2}\frac{y_{tip} - y_i}{\left(x_i - x_{tip}\right)^2} \tag{6.31}$$

$$\theta_{i,y} = \frac{1}{1 + \left(\frac{y_i - y_{tip}}{x_i - x_{tip}}\right)^2}\frac{1}{\left(x_i - x_{tip}\right)} \tag{6.32}$$

Finally the derivatives of the crack tip enrichment function with respect to the global coordinate system can be written as

$$\emptyset_{k,x} = \emptyset_{k,r}r_{i,x} + \emptyset_{k,\theta}\theta_{k,x} \tag{6.33}$$

$$\emptyset_{k,y} = \emptyset_{k,r}r_{k,y} + \emptyset_{k,\theta}\theta_{k,y} \tag{6.34}$$
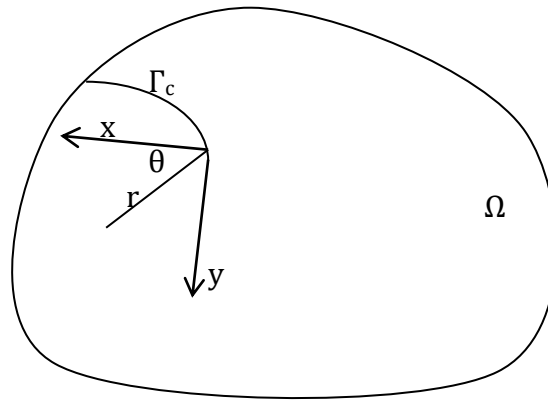
Figure 6.2 Polar Coordinate near the crack tip

6.2 Numerical Integration

The Gauss quadrature rule is widely used in finite element analysis for the numerical integration of stiffness matrix and other integral evaluation over a given domain. For the polygonal integrand the gauss quadrature is proved to be more accurate. In case of non-polygonal integrand it may result with some errors. Thus it may result some substantial accuracy reduction in output. For better results of numerical integration of more and more Gauss points are required. Less number of Gauss point may cause the various unavoidable errors.

Gauss Integration scheme is only applicable to the continuous function and over a continuous domain. In the presence of discontinuity, this numerical scheme get fails. This is further complicated as the crack path turns to be substantially curved. As a result, an efficient approach is required to define the necessary points needed for the integration points within the enriched element. This scheme has to be consistent with the geometry of the crack as well the order of the enrichment functions.

Because ordinary gauss rule do not calculate the integration of enrichment element. Dolbow [56] has proposed two methods to overcome the numerical integration difficulty. He talked about the portioning of the enriched element. He proposed that an enriched element can be sub-divided into the sub-triangles or the in the sub-quds.

6.2.1 Partitioning of element

An enriched element can be sub- divided into sub triangles or into the sub-quads. These two approaches are available for the improvement of the numerical integration. These two methodologies are described as below.

Sub-quads

In this method

- The element domain is uniformly partitioned into a regular subgrid of quadrature elements (sub-quads)
- Each sub-quad is assigned a predefined set of gauss quadrature points and corresponding weight function.
- The integrand and weight functions are computed at each gauss point.
- The final solution of the integral is obtained from the summation over all gauss points within the elements.
- A node is enriched only if there exists at least one Gauss point both side of the crack.

Sub-Triangles

This is an alternative to sub-quad approach by construction of local mesh of the triangular quadrature elements between the crack and element boundaries.

- Determine whether the crack crosses the element
- If the area between the crack and the corner node is very small compare to the element area, neglect the presence of crack and avoid the sub-triangulation
- Use a simple triangulation technique by adding a limited predefined numbers of the points inside an element and on its boundaries and connecting them t form consistent well shaped triangles
- A local Delaunay triangulation scheme may always be used as an automatic approach for the creation of quadrature sub-triangles.
- Each sub-triangle is assigned a predefined set of gauss points and corresponding weight function.
- The integrand and the weight function are computed at the every Gauss point.
- The final solution of the integral is obtained from the summation over all the gauss point within the element.

Figure 6.3 Partitioning of the element

6.3 Selection of Enriched Node

In the proposed methodology of GFEM, the approximation is enriched at the local level and it confined to the discontinuous domain. It means that selection of node to be enriched is an issue. There are various different ways to select a node for the enrichment process. Fig.6.4 shows the simple procedure to select the node for enrichment. At the each stage of propagation of the crack, nodes of that element will get enriched. If a crack touches the boundary of one element but does not go inside that element, then nodes of that element will not be enriched as shown in the Fig.6.4 (c).

(a)

(b)

(c)

(d)
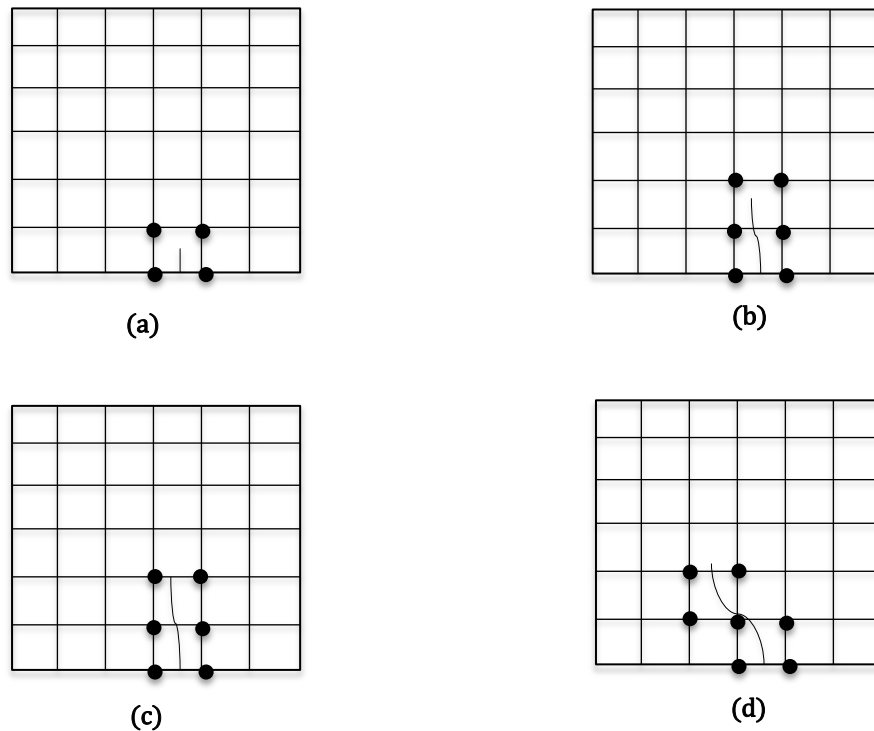
Figure 6.4 Enriched node at different stage of crack propagation (Black dot shows the enriched node)

The technique adds some additional degree of freedoms per node. The numbers of additional degree of freedoms depends on the choice of enrichment function (i.e. Heaviside function, crack-tip enrichment function or level set). Selection of the enrichment function is discussed in the next section.

6.3.1 Criterion for Node enrichment

1. First criterion is based on the area enclosed by the discontinuity. Fig. 6.5 (a) shows the area distribution with discontinuity. If the value of area ratio $\frac{A^+}{A^+ + A^-}$ is less than 0.01% then that node may not be enriched. If area ratio is more than 10% then the enrichment of node is compulsory.
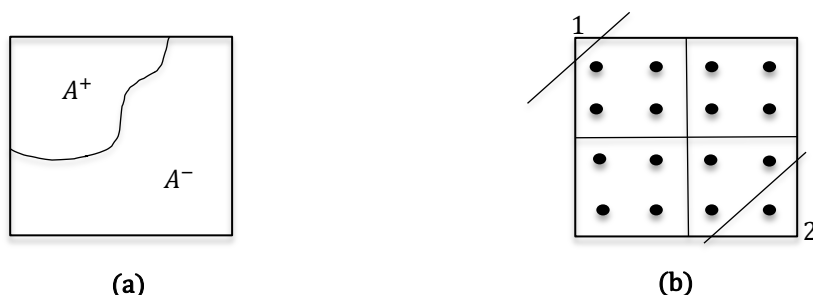
Figure 6.5 (a) description of area (b) existence of gauss point

2. Second criterion is based on the location of gauss point within the elements. According to this criterion if the gauss point is enclosed by the crack domain, then corresponding Node has to be enriched. If it's not enclosed, we have freedom for not enriching that node. As shown in the Fig.6.5 (b) gauss point corresponding to node 1 is outside the cracked domain, hence it gives freedom for enriching the node while Gauss point corresponding to node 2 is inside the domain. It's compulsory to enrich the node 2.

6.4 Assembly of the Global stiffness matrix

In classical FEM we assemble the nodal displacement vector based on the node numbers. In case of 2-dimensional problem the rth node will contribute for the (2r-1) and (2r) degree of freedom in the global matrix.

$$u = [u_1\ u_2\ \dots\dots u_{2r-1}\ u_{2r}\ \dots\dots u_n]$$

Same node will be responsible for (2r-1) & (2r) rows and column in the global stiffness matrix. It's always easy to implement it. In the case of GFEM, there are some additional degrees of freedoms. Now the challenge is that how to assemble these degrees of freedoms in the global stiffness matrix.

To assemble the additional Dofs, we have used the concept of the phantom nodes. These are virtual nodes and have no physical understanding. These are some random nodes which have numbered just after the number of real nodes. Number of phantom nodes depends on the type of enrichment function as well as the number of enrichment functions.

- The 1-Phantom Node is required for Heaviside-Enriched Element
- 4- Phantom Node is required for crack tip Enriched Element

6.5.1 Example of Phantom node implementation

Suppose a set of node N= [1, 2, 3, 4, 5, 6, 7] is given, In which the node number [3, 5,7] are Heaviside enriched and node [6] is enriched with the help of crack tip enrichment functions. A matrix of size 1*7 (ADN= [0, 0, 0, 0, 0, 0, 0]) is created. This ADN matrix is then updated according to the enrichment function and number of phantom or additional nodes. In this case after assigning the global number to the phantom doffs the ADN matrix will become ADN= [0, 0, 8, 0, 9, 10, 14]. Node number 3 and 5 are Heaviside enriched hence a next number is assigned to these places. Node number 6 is enriched by crack tip enrichment function; hence it required four phantom numbers. Due to presence of crack tip enrichment at node 6 next enriched nodes (i.e.7) got the global number as 14 (i.e. 9+4+1=14). Now the displacement vector will become as follows

$$u = [u_1 \ u_2 \ \ldots \ldots u_{2r-1} \ u_{2r} \ \ldots \ldots u_n \ a_3 \ a_5 \ b_6 \ a_7]$$

Where u_i is the nodal displacement at node, a_i is the additional dofs at the ith node due to Heaviside enrichment, b_i is the additional dofs at the ith node due to crack-tip enrichment

6.6 Conclusion

Detailed formulation of governing equation has been derived in this chapter. This formulation is done for enriched approximation. Numerical implementation issues are discussed in this chapter. Numerical integration and assembly of the global stiffness matrix has been illustrated with the help of an example. The concept of phantom node has been described with example.

Chapter 7

Numerical Example: Stress Analysis and SIF Study

7.1 Problem definition

In order to check and validate the robustness and efficiency of the proposed two scales GFEM, standard problems of the fracture mechanics has been solved as numerical examples. We have considered a 2-D plate with dimension L = 35 units, B = 15 unit. Young's modulus has been taken as $E = 1000000$ units, Poission's ratio is $v = 0.33$. Edge crack and inclined crack fracture problems have been illustrated the efficiency of the Multiscale GFEM. Plane stress condition has been considered with thickness of 1 unit.

A 4-noded bilinear element has been used for the discretization of the domain. The approximation of bilinear element is enriched with the help of the Heaviside function and crack tip enrichment function. 4 crack tip enrichment function has been used. Due the presence of the crack tip enrichment function and Heaviside function, the size of the element stiffness matrix increases from the classical 8*8 to 48*48. There is an increment of the 40 rows and column in each enriched element. Similar effects are in In case of blending element, all the nodes are not enriched. Classical nodes add numerical instability in global stiffness matrix by addition of zero rows and column. This instability has been improved by the elimination method. Rows and columns corresponding to the additional dofs of classical nodes within the blending element are eliminated from the global stiffness matrix.

7.2 Modeling 2-D Edge Crack Problem

A 2-dimensional plate with the dimension L = 35 units, B = 15 units has been considered for an edge crack problem. Crack length has been taken as $a = 7.5$ units. Domain dimensions and the Boundary conditions are shown in the Fig.7.1 (a). Edge crack is located at the mid height of the plate. Top edge of the plate has been given the displacement of $\delta = 8$ units. Bottom edge is constrained in the Y-direction. The bottom node on the right side is also constrained in the X-direction to prevent the rigid body motion in the X-direction.

Figure 7.1 (a) Edge Crack Problem (b) Inclined Crack Problem

7.2.1 Elastic Analysis

For an elastic analysis of the material properties has been taken as Young's modulus $E = 1000000$ units, and Poission's ratio $v = 0.33$. The problem has been solved using 4-noded quad element approximation. Fig.7.2 shows the contour plot of the stress in Y-direction and X-direction respectively.

σ_{yy} Plot $\qquad$ σ_{xx} Plot $\qquad$ σ_{xy} Plot

Figure 7.2 Stress Plot for Elastic Analysis of an Edge Crack Problem

48
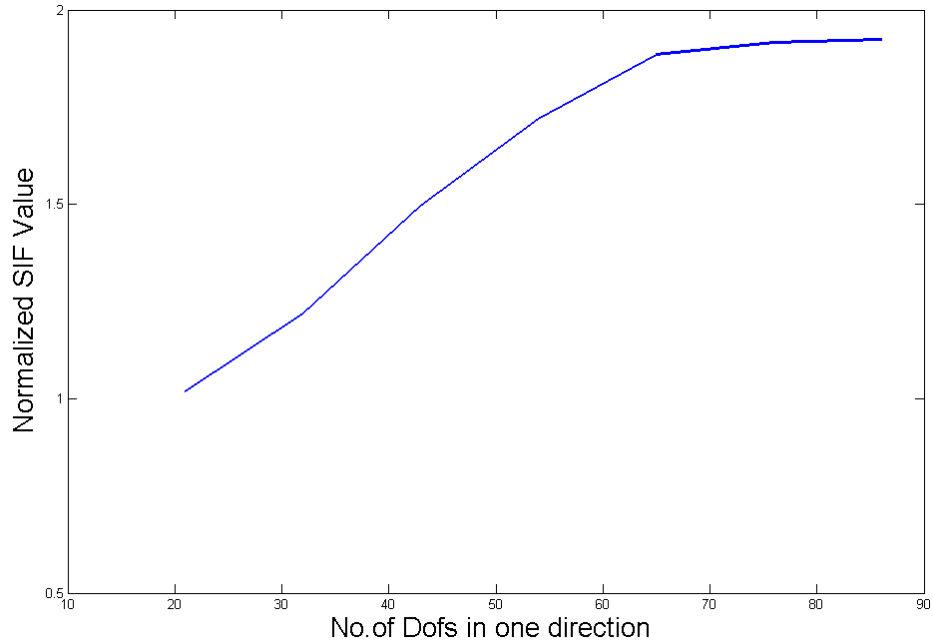
(Note: Normalized SIF= $\frac{K_I}{\sigma\sqrt{\pi a}}$ and Number of Dofs in one direction is =$\sqrt{2 * total\ Number\ of\ nodes}$)

Figure 7.3 Mesh Independency Study

In order to say that proposed method is mesh independent, we have done the Stress Intensity Factor (SIFs) evaluation with different meshes. Fig. 7.3 shows that there is an increment in normalized SIF with the increment of the number of degrees of freedoms in the domain. But this increment is not so large. It becomes a flat curve after a certain number of degrees of freedoms. Observation indicates that proposed method took a very small number of the elements as compare to the classical FEM analysis of the fracture problems. It can be concluded that the developed method is mesh independent. It's not a mesh free method but it's a mesh independent methodology.

7.2.2   Hyper-elastic Analysis

Mooney-Rivlin material model has been used for simulating the edge crack problem with the help of GFEM. Mooney-Rivlin is a hyper elastic material model in which the strain energy is defined as the linear combination of the two invariant of the left Cauchy's Green deformation tensor. This method was proposed by Melvin Mooney in 1940 and expressed as a linear combination of invariant in 1948 by Ronal Rivlin.

49

Constitutive relation to Hyperelastic Analysis:

A quadratic isotropic function of the Green strain tensor $E = \frac{1}{2}(C - 1)$ can be used to define the constitutive relation. From the St. Venant material principle the stored energy can be written as

$$W = \frac{\lambda}{2}(trE)^2 + \mu tr(E)^2$$

Where λ and μ are Lame's parameters. We can simplify this expression to

$$W = C_1(\overline{I_1} - 3)$$

The strain energy density function for Mooney Rivlin can be written as

$$W = C_{10}(\overline{I_1} - 3) + C_{01}(\overline{I_2} - 3)$$

Where $\overline{I_1}$ and $\overline{I_2}$ are first and second invariant of the unimodular component of the left Cauchy-Green deformation tensor. These invariants are defined in term of stress invariant I_1 and I_2.

$$\overline{I_1} = J^{-2/3}I_1$$
$$\overline{I_2} = J^{-4/3}I_2$$

Where the constant $J = 1$ for incompressible material

Most generalized forms of the strain energy density with the effect of compressible material can be rewritten as

$$W = C_{10}(\overline{I_1} - 3) + C_{01}(\overline{I_2} - 3) + D_1(J - 1)^2$$

The hydrostatic pressure can be correlated with energy density function as follows

$$P = \frac{\partial \widetilde{W}}{\partial J} = -K(J - 1)$$

The hyperelastic analysis is based on the incremental stress and very large deformation. Incremental stress can be written as

$$\Delta S_{ij} = C_{ijkl}\Delta E_{kl} + g_{ij}\Delta P$$

Where C_{ijkl} and g_{ij} are material response tensor of 4th order and 2nd order respectively, S_{ij} is Piola-Kirchoff stress. These tensors can be written as

$$C_{ijkl} = \bar{C}_{ijkl} + \tilde{C}_{ijkl} = \frac{\partial^2 W}{\partial E_{ij}\partial E_{kl}} + \frac{\partial\left(-JG_{ij}^{-1}\right)}{\partial E_{kl}}P$$

$$g_{ij} = -\frac{I^{1/2}}{3}G_{ij}^{-1}$$

The explicit expression of $\bar{C}_{ijkl}$, $\tilde{C}_{ijkl}$ are as below

$$\bar{C}_{ijkl} = \frac{\partial^2 W}{\partial E_{ij} \partial E_{kl}}$$

$$= \left(\frac{4}{3}C_{10}I_3^{-\frac{1}{3}}I_1 + \frac{16}{9}C_{01}I_3^{-\frac{2}{3}}I_2\right)G_{ij}^{-1}G_{kl}^{-1} - \left(\frac{4}{3}C_{10}I_3^{-\frac{1}{3}} + \frac{8}{3}C_{01}I_3^{-\frac{2}{3}}\right)\left(\delta_{ij}G_{kl}^{-1} + G_{ij}^{-1}\delta_{kl}\right)$$

$$+ \left(\frac{2}{3}C_{10}I_3^{-\frac{1}{3}}I_1 + \frac{4}{3}C_{01}I_3^{-\frac{2}{3}}I_2\right)\left(G_{ik}^{-1}G_{jl}^{-1} + G_{il}^{-1}G_{jk}^{-1}\right) + 4C_{01}I_3^{-\frac{2}{3}}\delta_{ij}\delta_{kl}$$

$$- 2C_{01}I_3^{-\frac{2}{3}}\left(\delta_{ik}\delta_{jl} + \delta_{il}\delta_{jk}\right) + \frac{8}{3}C_{01}I_3^{-\frac{2}{3}}\left(G_{ij}\,G_{kl}^{-1} + G_{ij}^{-1}G_{kl}\right)$$

$$\tilde{C}_{ijkl} = \frac{\partial\left(-JG_{ij}^{-1}\right)}{\partial E_{kl}}P = PJ\left(G_{ik}^{-1}G_{jl}^{-1} + G_{il}^{-1}G_{jk}^{-1} - G_{ij}^{-1}G_{kl}^{-1}\right)$$

$$g_{ij} = -I_3^{1/2}G_{ij}^{-1}$$

Where G_{ij}^{-1} is the ij th component of the G^{-1}

The same problem of elasticity analysis has been usedinr the hyper-elastic analysis of the edge crack problem. The coefficient of the strain energy function has been taken as $C_{10} = 0.293, C_{01} = 0.177$ units, $D_1 = 10 = 0.5k$. Where k is the bulk modulus. The stress plots of hyper-elastic analysis are shown in the Fig. 7.4
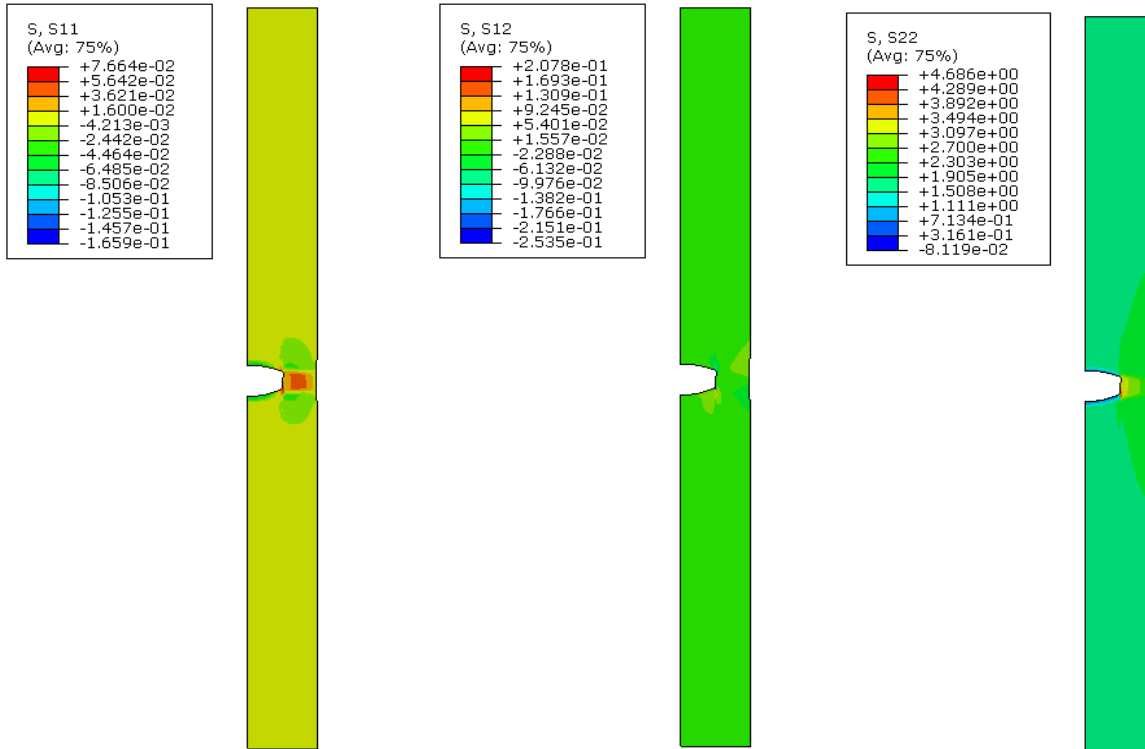
Figure 7.4 Stress Plot for Hyper-elastic Analysis of Edge Crack Problem

7.3 Modeling 2-D Inclined Crack Problem

A 2-dimensional plate with the dimension $L = 35$ units, $B = 15$ units has been considered for an edge crack problem. Crack length has been taken as $a = 7.5$ units. Domain dimensions and the Boundary conditions are shown in the Fig.7.1 (b). Crack is located at the mid of the plate. Top edge of the plate has been given the displacement of $\delta = 10$ units. Bottom edge is constrained in the Y-direction. The bottom node on the right side is also constrained in the X-direction to prevent the rigid body motion in the X-direction.
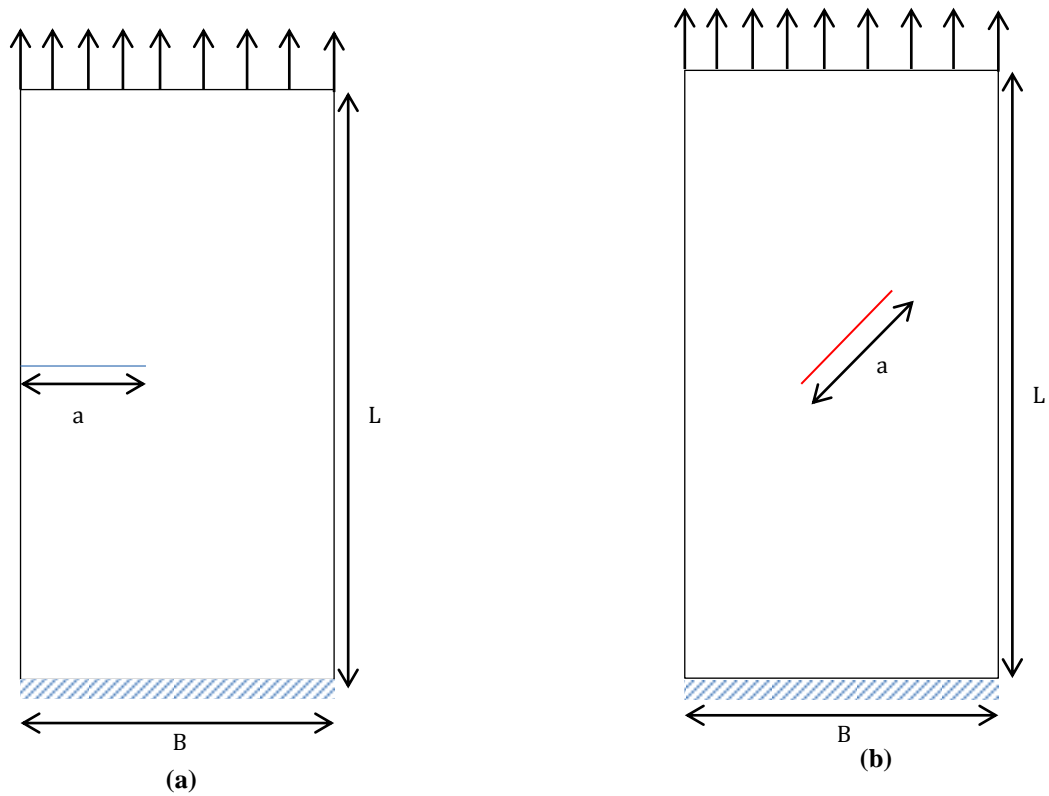
7.3.1   Elastic Analysis

For an elastic analysis of the material properties has been taken as Young's modulus $E = 1000000$ units, and Poission's ratio $v = 0.33$. The problem has been solved using 4-noded quad element approximation. Fig. 7.5 shows the contour plot of the stress in X-direction, XY-direction and Y-direction respectively.
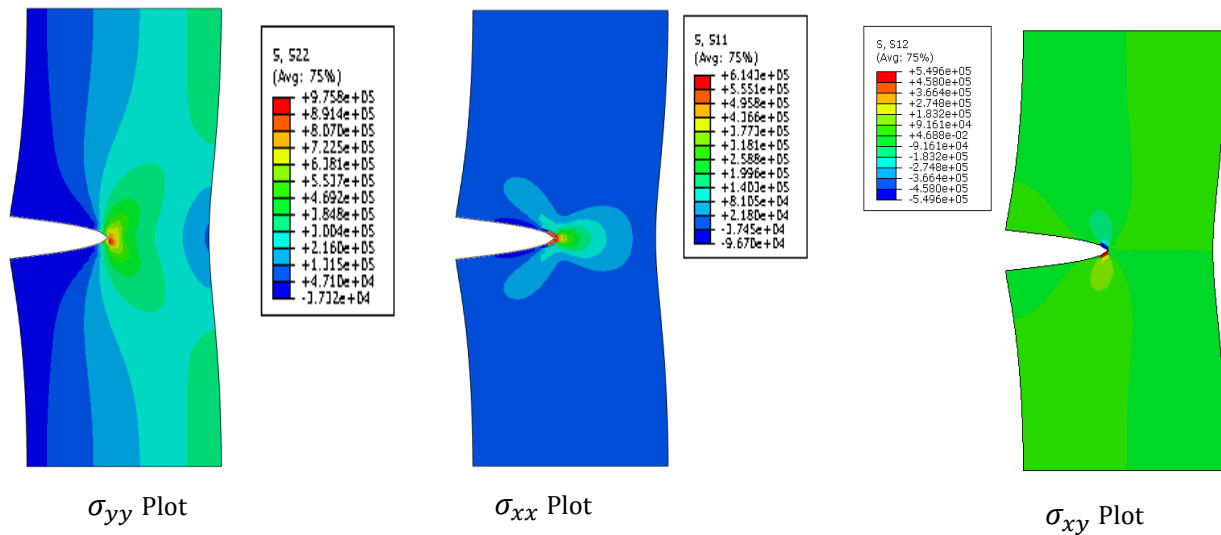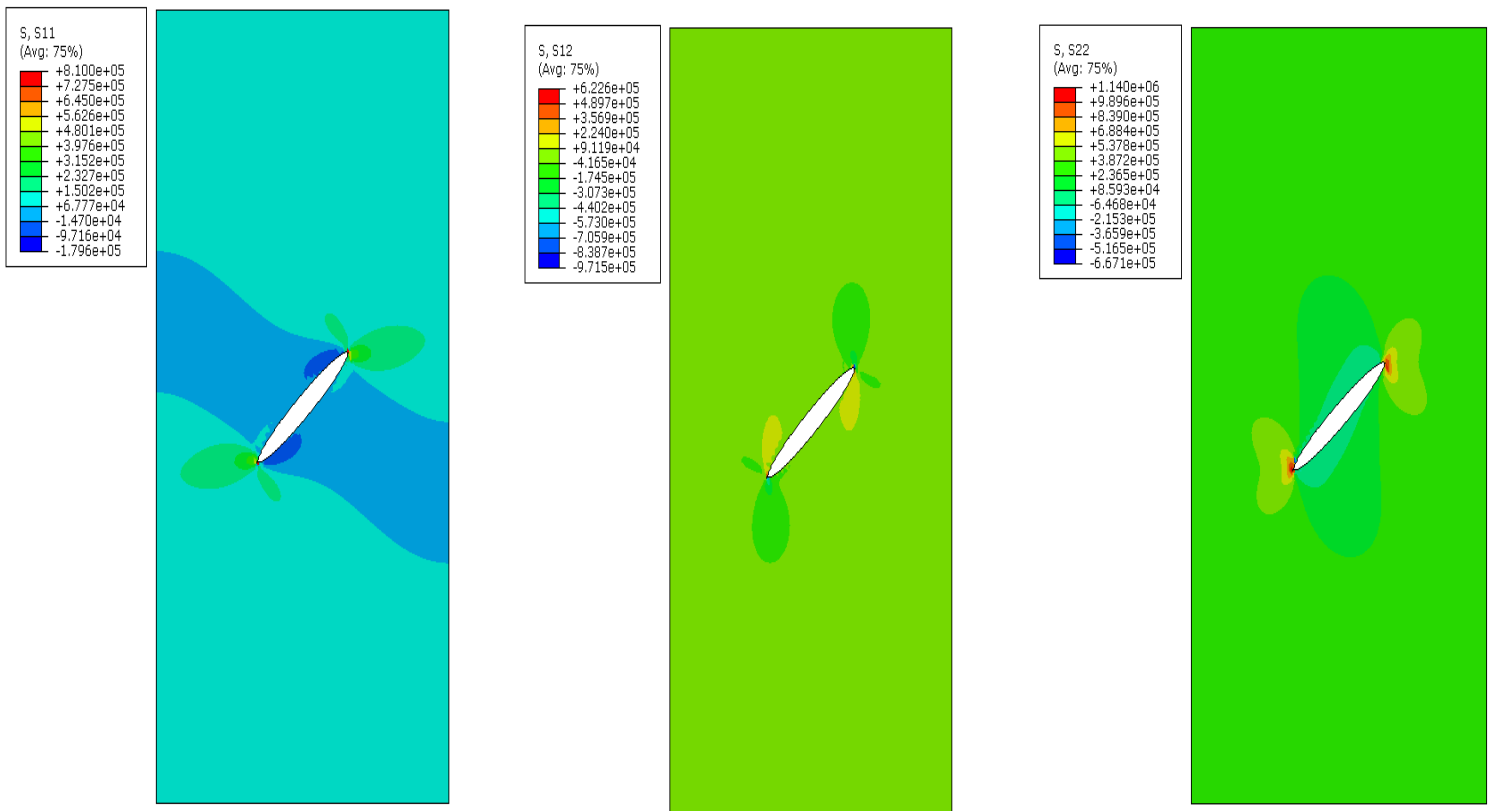

Figure 7.5 Stress Plot for Elastic Analysis of an Inclined Crack Problem

7.4 Conclusion

In the present chapter, numerical examples were illustrated. Capability and the potential of the GFEM have been illustrated with edge crack and inclined crack problem. Observation of the results indicates to optimal and efficient simulation tool. It can be concluded that the developed tool requires a very coarse mesh to capture the complex geometries. Adaptive remeshing is also not mandatory. It also infers that discrete cracks are not required for modeling static crack. Mesh independency has been studied through the SIF study with respect to the various mesh sizes.

Chapter 8

Sensitivity Analysis

8.1 Introduction

Sensitivity analysis of a solution is the measurement of the uncertainty in the output. It is based on variational formulation of the continuum mechanics. Structural optimization and sensitivity analysis has become most popular research field over a decade. Main objective of these kinds of studies is to get most economical optimized and efficient design. It has wide and enormous application in automobile industry, aerospace industry, civil structures and many more. It became reliable also due to presence of better simulation tools. Most of these simulation tools are in-built with the finite element analysis and with different post processing tools.

8.2 Literature Survey

Bugeda et al. [42] had introduced the methodology for shape sensitivity analysis and they talked about the shape optimization. Their methodology was based on adaptive mesh refinement. They had validated their methodology with the help of B-spline functions defined at the boundaries. They have studied the optimal shape design by controlling the errors and minimizing the same. An error has been controlled by the means of finite element or boundary element motion and converting the shape derivatives into differentiations of algebraic equations [43].

Another approach for sensitivity analysis is based on a variational formulation of the continuum mechanics [44, 45]. In this approach shape sensitivity is simulated with the help of the velocity field. This velocity field is responsible for the shape change of the body which applies to initial domain. Taroco [46] had given mathematical formulation of the shape sensitivity analysis in linear elastic fracture problems. He had established the relation between the domain and boundary expressions for the first and higher order derivatives of the potential energy stored in elastic body with respect to the shape change.

Chen et. al [47] has illustrated the shape sensitivity analysis of the elastic body with mode-I fracture problem. B. N. Rao [48] has considered the functionally graded material to demonstrate the capability of the variational formulation of the sensitivity analysis. He had done the sensitivity analysis for all the

54

modes of fracture failure. Very recently, Edke et. al [49] has implemented the same formulation for the extended FEM with the level set function as the enrichment function.

8.3 Velocity field

Consider a 3 –dimensional body with domain Ω and boundary Γ and body material point have position vector $x \in \Omega$. Assume that at time T=τ body will have domain Ω_τ and boundary Γ_τ as shown in Fig.8.1.
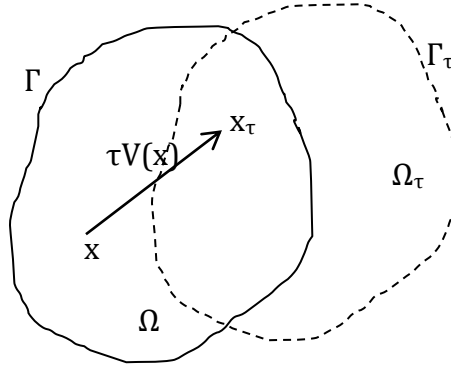
Figure 8.1 Variation of the domain

Movement from one place to another place can be expressed as

$$T: x \rightarrow x_\tau, x \in \Omega \qquad (8.1)$$

Where x, x_τ are position vectors at different time.

If T is the transformation mapping, and τ is the scalar time with the parameters of shape change

$$x_\tau = T(x, \tau) \qquad (8.2)$$

$$\Omega_\tau = T(x, \tau) \qquad (8.3)$$

$$\Gamma_\tau = T(x, \tau) \qquad (8.4)$$

A velocity field can be defined as

$$V(x, \tau) = (dx_\tau)/d\tau = (dT(x, \tau))/d\tau = (\partial T(x, \tau))/\partial \tau \qquad (8.5)$$

Using Taylor's expansion and ignoring the higher order terms the transformation mapping can be approximated by

$$T(x, \tau) = T(x, 0) + \tau \frac{\partial T(x,0)}{\partial \tau} + O(\tau^2) \cong x + \tau V(x, 0) \qquad (8.6)$$

There are lots of different methods to define the velocity field [50]. For an edge crack problem we have considered the velocity variation as shown in the Fig.8.2.

Consider a plate with a horizontal crack with the dimension of L*B. Though we had symmetry but we had modeled full plate as shown in Fig. 8.4. A PQRS domain has been considered as the domain for the calculation of J-integral and its sensitivity. The size of this domain is $((2*l_1)*(2*b_1))$, which enclosed the crack tip inside it as shown in the Fig. 8.2.

The velocity field used in this study has been defined as

$$V(x) = \begin{cases} V_1(x) \\ V_2(x) \end{cases} = V_{1,tip} \begin{cases} A_1(x_1)A_2(x_2) \\ 0 \end{cases} \tag{8.7}$$

Where

$$A_1(x_1) = \begin{cases} 1, & if \ |x_1| \leq 0.5b_1 \\ \dfrac{x_1-B+a}{b_1-B+a} & if \ x_1 \geq b_1 \\ \dfrac{x_1+a}{b_1+a} & if \ x_1 \leq -b_1 \end{cases} \tag{8.8}$$

$$A_2(x_2) = \begin{cases} 1, & if \ |x_2| \leq 0.5l_1 \\ \dfrac{x_1-B+a}{b_1-B+a} & if \quad L > x_2 > 0.5l_1 \\ 0 & if \ x_2 > L \end{cases} \tag{8.9}$$
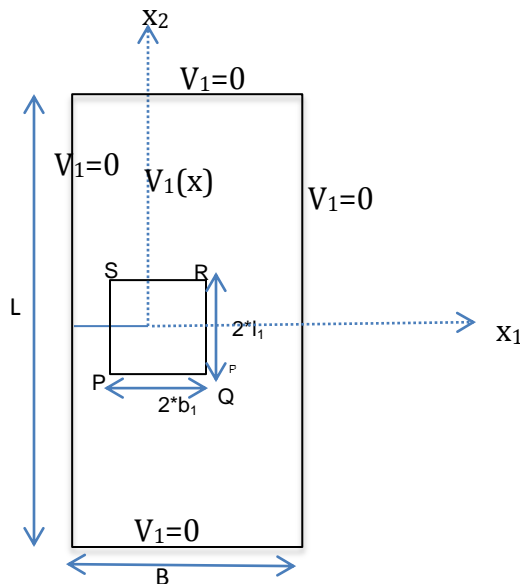
Figure 8.2 Schematic diagram of velocity field in the domain

7.4 Sensitivity Analysis

The variational form of the governing equation can be written as [51]

$$b_A(u, \bar{u}) = l_A(\bar{u}) \qquad \forall \, \bar{u} \in U \qquad\qquad (8.10)$$

Where $\bar{u}$ and U are actual displacement and virtual displacement of the structures and

$$b_A(u, \bar{u}) = \int \sigma_{ij}(u) \, \varepsilon_{ij}(\bar{u}) d\Omega \qquad\qquad (8.11)$$

$$l_A(\bar{u}) = \int f_i^b \bar{u}_i d\Omega + \int_\Gamma T_i \bar{z}_i d\Gamma \qquad\qquad (8.12)$$

7.4.1 Material derivative

For a given point $x \in \Omega$, material derivative a is expressed as [51]

$$\dot{u} = \lim_{\tau \to 0} \left[\frac{u_\tau(x + V(x)) - u(x)}{\tau} \right] \qquad\qquad (8.13)$$

If the u_τ continuous, then it can be extended in the neighborhood of Ω.

$$\dot{u}(x) = u'(x) + \nabla u^T V(x) \qquad\qquad (8.14)$$

Where $u' = \lim_{\tau \to 0} \left[\frac{u_\tau(x) - u(x)}{\tau} \right]$

Material derivative has commutative properties i.e $\left(\frac{\partial u}{\partial x_x} \right)' = \frac{\partial}{\partial x_x}(u')$

7.4.2. Variational formulation

Lets assume a domain functional $\emptyset_1$ defined over the domain Ω. In the integral form it can be expressed as

$$\emptyset_1 = \int_\Omega f_\tau(x_\tau) d\Omega_\tau \qquad\qquad (8.15)$$

Where f_τ is regular function over the domain Ω and domain Ω is C^k regular. For assumed functional material derivative [51] can be written as

$$\dot{\emptyset}_1 = \int_\Omega [f'(x) + div(f(x)V(x))] d\Omega \qquad (8.16)$$

For the functional form of $\emptyset_2 = \int_{\Omega_\tau} g(u_\tau, \nabla u_\tau) d\Omega_\tau$

The material derivative of $\emptyset_2$ in domain Ω can be written as in

$$\dot{\emptyset}_2 = \int_\Omega \left[g_{,u_i}\dot{u}_\iota - g_{,u_i}(u_{i,j}V_j) + g_{,u_i}\dot{u}_{\iota,J} - g_{,u_{i,j}}(u_{i,j}V_j)_{,j} + div(gV) \right] d\Omega \qquad (8.17)$$

If no body force is equal to zero then the variational equation (8.10) can be re-written as

$$b_A(u,\bar{u}) \equiv \int \sigma_{ij}(u)\,\varepsilon_{ij}(\bar{u})d\Omega = l_A(\bar{u}) \equiv \int_\Gamma T_i \bar{z}_i d\Gamma \qquad (8.18)$$

Taking the material derivative of the equation (8.18) and using equations (8.13, 8.14)

$$b_A(u,\bar{u}) = l_A{}'(\bar{u}) - b_V'(u,\bar{u}) \qquad \forall\,\bar{u} \in U \qquad (8.19)$$

Where V denotes the velocity dependency.

$$l_A{}'(\bar{u}) = \int_\Gamma \left\{ -T_i(u_{i,j}V_j) + \left[(T_i\bar{u}_i)_{,j}n_j + k_\Gamma(T_i\bar{u}_i) \right](V_i n_i) \right\} d\Gamma \qquad (8.20)$$

$$b_V'(u,\bar{u}) = \int_\Omega \left[\sigma_{ij}(u)(\bar{u}_{i,k}V_{k,j}) + \sigma_{ij}(\bar{u})(u_{i,k}V_{k,j}) - \sigma_{ij}(u)\varepsilon_{ij}(\bar{u})divV \right] d\Omega \qquad (8.21)$$

Where n_j is the jth component of unit normal to domain, k_Γ is the curvature of the boundary.

8.4.3 Sensitivity of J-Integral

In the absence of the body force, equation (3.23) can be rewritten as

$$J = \int_\Omega \left[\sigma_{ij}\frac{\partial u_j}{\partial x_1} - W\delta_{1j} \right]\frac{\partial q}{\partial x_i} d\Omega \qquad (8.22)$$

Where δ_{1j} is Kronecker delta, q is an arbitrary weight function, which varies linearly from zero to one. Ω is the enclosed area by the contour Γ. Equation (8.22) can be expanded further as

$$J = \int_\Omega \left[\left(\sigma_{11} \frac{\partial u_1}{\partial x_1} + \sigma_{12} \frac{\partial u_2}{\partial x_1} \right) \frac{\partial q}{\partial x_1} + \left(\sigma_{21} \frac{\partial u_2}{\partial x_1} + \sigma_{22} \frac{\partial u_2}{\partial x_1} \right) \frac{\partial q}{\partial x_1} - W \frac{\partial q}{\partial x_1} \right] d\Omega \qquad (8.23)$$

For 2-dimensional problem (i.e. plane stress, plane strain) the equation (8.23) can be written as

$$J = \int_\Omega g\, d\Omega \qquad (8.24)$$

Where $g = g_1 + g_2 + g_3 + g_4 - g_5 - g_6$. The explicit expressions of m_i can be found in Appendix-I.

A material derivative of the J-integral can be written as

$$\dot{J} = \int_\Omega [g' + div(gV)] d\Omega \qquad (8.25)$$

Where $g' = g_1' + g_2' + g_3' + g_4' - g_5' - g_6'$

V is the velocity field. It has been described in the section 8.3 and schematic diagram of the velocity variation is shown in the Fig. 8.2. Assuming the crack length a as variable increasing in the direction x_1. The expression of equation (8.25) can be rewritten as

$$\dot{J} = \int_\Omega (G_1 + G_2 + G_3 + G_4 - G_5 - G_6) d\Omega \qquad (8.26)$$

Where $G_i = g_i' + div(g_i V)$ $\qquad i = 1,2,3, \ldots 6$

The formula for g_1 and G_1 is given below

$$g_1 = \frac{E}{1-v^2} \frac{1}{2} \left(\sum N_{i,x} u_i + \sum N_{i,x} \sum \emptyset_k b_{ik} + \sum N_i \sum \emptyset_{k,x} b_{ik} \right)^2 \frac{\partial q}{\partial x_1}$$

$$G_1 = \frac{E}{1-v^2} \frac{\partial q}{\partial x_1} \left[\left(\sum N_{i,x} u_i + \sum N_{i,x} \sum \emptyset_k b_{ik} + \sum N_i \sum \emptyset_{k,x} b_{ik} \right) \frac{\partial \dot{u}_1}{\partial x_1} \right.$$
$$\left. - \left(\sum N_{i,x} u_i + \sum N_{i,x} \sum \emptyset_k b_{ik} + \sum N_i \sum \emptyset_{k,x} b_{ik} \right)^2 \frac{\partial V_1}{\partial x_1} \right]$$

The explicit expressions of other G_i are given in Appendix-II.

59

8.4.4 Flow chart


```
                    ( Start )
                        |
                        v
  +-------------------------------------------+
  |   Solve the bilinear form using GFEM and  |
  |        get the displacement u             |
  |                                           |
  |          b_A(u, ū) = l_A(ū)               |
  +-------------------------------------------+
                        |
                        v
  +-------------------------------------------+
  |  Solve the bilinear form using GFEM and in|
  |   order to get the material derivative u̇  |
  |                                           |
  |     b_A(u̇, ū) = l_V(ū) − b_V(u̇, ū)        |
  +-------------------------------------------+
                        |
                        v
  +-------------------------------------------+
  |  Compute the function G₁, G₂, G₃..... G₆  |
  +-------------------------------------------+
                        |
                        v
  +-------------------------------------------+
  |        Compute the sensitivity of J       |
  |                                           |
  |          j = Σⁱ₌₁ ∫ Gᵢ dA                 |
  +-------------------------------------------+
                        |
                        v
                    ( End )
```

Solve the bilinear form using GFEM and get the displacement u

$$b_A(u, \bar{u}) = l_A(\bar{u})$$

Solve the bilinear form using GFEM and in order to get the material derivative $\dot{u}$

$$b_A(\dot{u}, \bar{u}) = l_V(\bar{u}) - b_V(\dot{u}, \bar{u})$$

Compute the function G_1, G_2, G_3..... G_6

Compute the sensitivity of J

$$j = \sum_{i=1}^{6} \int G_i dA$$

Figure 8.3 Flow chart of the sensitivity analysis

8.4.5 Numerical example

We have considered an edge crack problem as shown in Fig. 8.4. A plate with dimension 35*15 units has been considered as the problem. The given plate has a crack of length a units. One loading condition has been considered as constant strains. Fig. 8.4 shows the schematic diagram of the problem with the loading conditions. Young's modulus of plate is uniform throughout the whole width as well as in whole length. The specifications and the numerical values of the problem are as follows:

    a. Young's Modulus, $E = 35$ unit

    b. Shear Modulus, $G = 26$ units

    c. Poisson's ratio $v = 0.33$

    d. Crack length $a = 7.5$ unit, (its different for different cases.)

    e. Domain dimension, $L * B = 35 * 15$ unit

    f. Dirichlet Boundary condition; $u_y = 1$ unit on top edge, $u_y = 0$ for bottom edge, $u_x = 0$ for bottom corner node
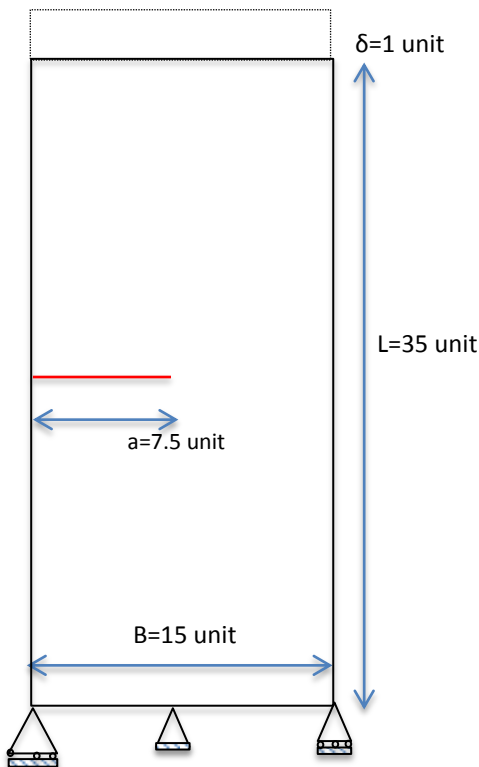
Figure 8.4 (a). Numerical example-I   **Figure 8.4 (b). Numerical example-II**   **Figure8.4 (c). Numerical example-III**
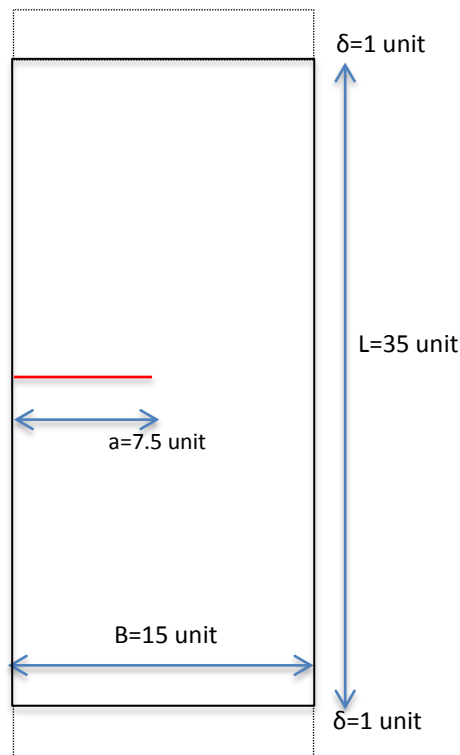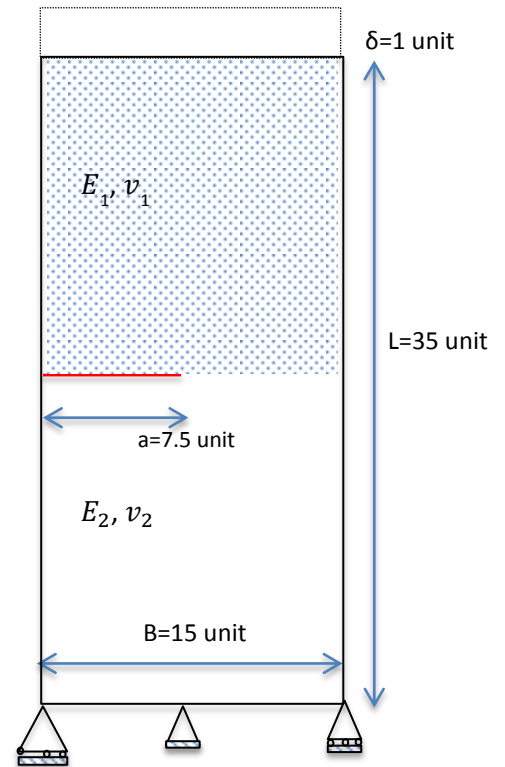
Full plate has been modelled for $\frac{a}{B} = 0.1, 0.2, 0.3, 0.5$ as shown in Fig 8.5 (a-b) respectively. 4- Node bilinear element has been used in the analysis. The domain has been discretized into the 78 elements and 112 elements for $\frac{a}{B} = 0.1$ and $\frac{a}{B} = 0.2, 0.3, 0.5$ respectively. Number of enriched elements depends on the a/B ratio, which directly impact on the total degree of freedom. As the size of element stiffness matrix is bigger than the classical stiffness matrix, hence the global stiffness matrix gets increased by some numbers. But the overall size of the global stiffness matrix is lesser than the required matrix size in classical FEM. By this we are benefiting in the storage space in the computer. Sensitivity of the crack length and stress intensity has been calculated all the given case.

(a)   (b)
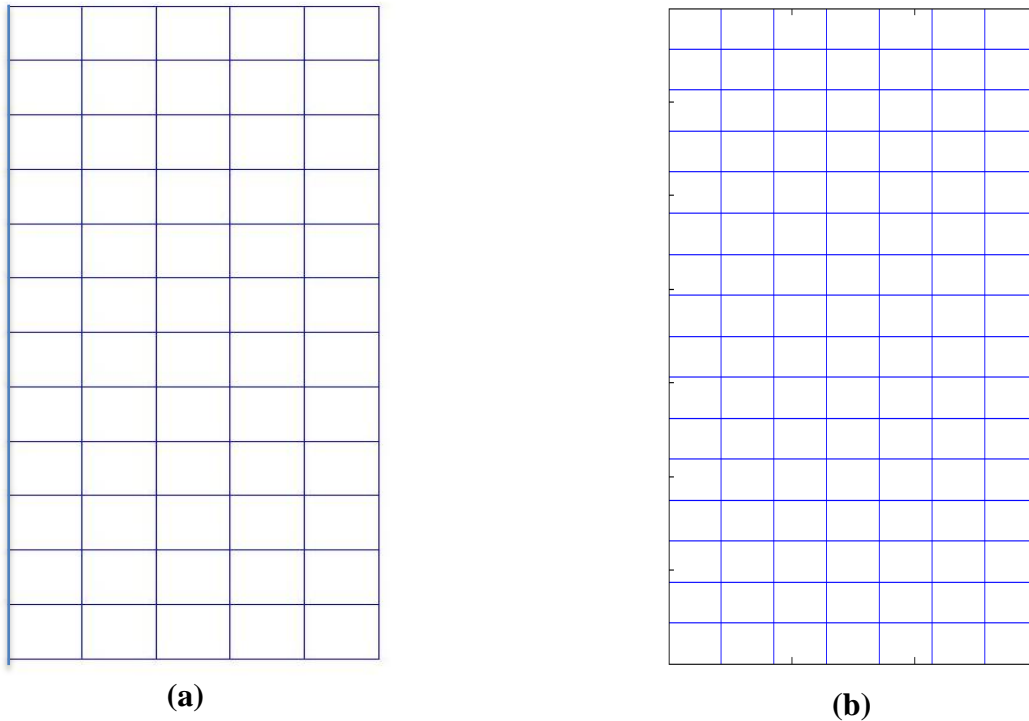
Figure 7.5 Finite element mesh for (a) a/B=0. 1   (b) for a/B=0. 2, 0.3, 0.5

SIF and sensitivity of J-integral has been calculated near the crack tip. A domain of $2l_1 * 2b_1$ has been considered for calculating the J-integral and its sensitivity for $\frac{a}{B} = 0.1, 0.2, 0.3, 0.5$.

8.4.6 Results and Discussion

All the tables contain the numerical results of the normalized SIF, sensitivity analysis of J-Integral by 2 various methods. The first method is based on the variational formulation method with GFEM and another method is the first principle of derivative. In the first method the crack length a is considered as the variable. The first order derivative is calculated with respect to the crack length. There is no analytical solution so for validation purpose we have adopted the differentiation technique. In differentiation we have considered the change in crack length. The first principle of differentiation is defined as the change in the value of the function with respect to the small change (tending to zero) in the independent variable. We have considered the change in the crack length as 4-6 % in each case.

Table-8.1 & 8.2 contains the numerical results of the example-I. Both plane stress and plane strain conditions are considered and analyzed for each state. There is no mesh change is required in both the methodology for the calculation of the J-Integral. In methodology same mesh had been used for finding the derivative of displacement and the material derivative of the displacement.

Table 8.1: Sensitivity Analysis for Edge crack problem: Plane Strain Condition (Numerical Example-I)

S.No.	a/B ratio	Normalized SIF	Sensitivity of J-Integral		Difference
			GFEM	Direct Method	
1	0.1	0.408390231	0.3273	0.36666667	-0.03937
2	0.2	1.46395224	0.2842	0.283333333	0.000867
3	0.3	1.517102374	0.3689	0.343333333	0.025567
4	0.5	1.266009715	0.5852	0.563333333	0.021867

Table 8.2: Sensitivity Analysis for Edge crack problem: Plane Stress Condition (Numerical Example-I)

S.No.	a/B ratio	Normalized SIF	Sensitivity of J-Integral		Difference
			GFEM	Direct Method	
1	0.1	0.405829765	0.258	0.243333333	0.014666667
2	0.2	1.46395224	1.346	1.336666667	0.009333333
3	0.3	1.516873325	1.503	1.473333333	0.029666667
4	0.5	1.265845031	1.954	2.153333333	-0.199333333

Numerical results of example-II are tabulated in the Table 8.3 & 8.4. These tables contain the numerical results of the SIF study and the sensitivity analysis of the J-Integral. In this case also plane stress and

plane strain conditions are applied for numerical simulations and results are tabulated in the different tables. Table 8.5 shows the results for a bimaterial plate which has young's modulus ratio $E_1/E_2 = 0.1$

The difference between the results of GFEM and the direct method is less than 3%. There is a big difference in the result for a/B =0.5 is due to formation of large plastic domain ahead of the crack tip. Direct method, which has been used here, required a very fine mesh for calculation of the J-Integral but here in this case we have taken a very coarser mesh.

Table 8.3: Sensitivity Analysis of Edge crack problem: Plane Strain Condition (Numerical Example-II)

| S.No. | a/B ratio | Normalized SIF | Sensitivity of J-Integral | | Difference |
			GFEM	Direct Method	
1	0.1	0.472154568	0.511068	0.49736	0.013708
2	0.2	0.636387763	0.156616	0.136666	0.01995
3	0.3	1.076678071	0.109261	0.110132	-0.00087
4	0.5	1.006032758	0.317538	0.333333	-0.0158

Table 8.4: Sensitivity Analysis for Edge crack problem: Plane Stress Condition (Numerical Example-II)

| S.No. | a/B ratio | Normalized SIF | Sensitivity of J-Integral | | Difference |
			GFEM	Direct Method	
1	0.1	0.472154568	0.09399	0.1005	-0.00651
2	0.2	0.635657541	0.4212	0.4333	-0.0121
3	0.3	1.076678071	0.4693	0.4700	-0.0007
4	0.5	1.006217402	1.6345	1.6066	0.0279

Table 8.5: Sensitivity Analysis for Edge crack problem: Plane Stress Condition (Numerical Example-III)

$E_1/E_2 = 0.1$

| S.No. | a/W ratio | Normalized SIF | Sensitivity of J-Integral | | Difference |
			GFEM	Direct Method	(%)
1	0.1	1.29606214	3.98	4.11	5.10
2	0.3	1.50902861	93.11	87.75	-5.73

Observation of the results

J-Integral is quantified parameters in the prediction of the fatigue life of the material. It depends on the various independent variables such as length of the crack, loading conditions, boundary conditions and the approximation schemes. The ratio of the crack length and width has a great role in terms of the optimization of the structures. Results show that J-Integral is very sensitive to the applied load, the geometry of the model and the analysis type.

Conclusion

A new method has been developed for sensitivity analysis of the discontinuity in elastic, isotropic, and homogeneous material using the GEFM as the tool for fracture analysis. The proposed method involves the material derivatives, displacement derivatives, J-Integral calculation. As all these steps are based on variation form, which required the discretization of the domain. Discretization is dominating step in the FEM analysis whereas this proposed method is based on the GFEM. GFEM has been shown a very advanced tool for fracture analysis. GFEM is meshfree tool. Hence the errors due to the discretization are minimized. The numerical results show that the difference between two methodologies is less than 4%.

Chapter 9

Conclusion

9.1 Summary and conclusion

GFEM is enrichment based method which is capable of the exactly capturing the stress state ahead of the crack tip. This methodology based on the enhancement of the classical approximation with help of enrichment function. Selection of the enrichment function is depends on the priori knowledge of the solution. These functions may be polynomial or non-polynomial function, discontinuous functions, singular function, and trigonometric functions. GFEM relies on the enrichment function from the POD modes of elastic solution.

In this work the GFEM was studied with enrichment from POD modes. Various enrichment functions have been studied in this work. Heaviside function, modified Heaviside function and partition of unity based function have been illustrated for 1-D domain as well as for the 2-D domain. Crack tip enrichment functions and level set based enrichment functions has been studied to capture the discontinuity.

Furthermore the mathematics of the GFEM has been rewritten in the context of the enriched approximation. Galerkin formulation and numerical integration schemes has been discussed in the documentation. Edge crack and inclined crack problem has been considered to illustrate the capability of the present work.

The developed matlab code has been used to perform the sensitivity analysis of the J-Integral. The mathematical model of the Sensitivity analysis has been derived. This mathematical model is based on the principle of the material derivate of continuum mechanics. Sensitivity analysis has been done for edge crack problem. A domain with two materials has been also entertained as another numerical example.

J-Integral has been considered as the dependent variable. Geometry of the domain, loading conditions, solution approximations have been considered as independent variables. The effects of these independent variables on the dependent variable have been tabulated in the sensitivity analysis. Furthermore the relation between two independent variable has been observed from the tabulated results.

9.2 Future work

GFEM has lots of potentials in terms of capturing the exact behavior and modeling the complex geometries. It has capability to predict the failure load behavior and also the post peak behavior. In spite of being such a capable tool, it has some limitations. Numerical integration is one of the main issues in the present work, which has to be studied in future.

GFEM can be used as a simulation tool for the coupled problems. It can be coupled with any damage criterion to predict the damage flow. It can be elaborated with the traction separation law for homogenization of the heterogeneous materials.

List of figures

List of the tables

Appendix-I

g Function for sensitivity analysis

Plane stress Condition

$$g_1 = \frac{E}{1-v^2} \frac{\varepsilon_{11}^2}{2} \frac{\partial q}{\partial x_1} \tag{1}$$

$$g_2 = \frac{E}{1+v} \varepsilon_{11} \frac{\partial u_2}{\partial x_1} \frac{\partial q}{\partial x_1} \tag{2}$$

$$g_3 = \frac{E}{1+v} \varepsilon_{12} \varepsilon_{11} \frac{\partial q}{\partial x_2} \tag{3}$$

$$g_4 = \frac{E}{1-v^2} (\varepsilon_{22} + v\varepsilon_{11}) \frac{\partial u_2}{\partial x_1} \frac{\partial q}{\partial x_2} \tag{4}$$

$$g_5 = \frac{E}{1+v} \varepsilon_{12}^2 \frac{\partial q}{\partial x_1} \tag{5}$$

$$g_6 = \frac{E}{1-v^2} \left(\frac{\varepsilon_{22}^2}{2} + v\varepsilon_{11}\varepsilon_{12} \right) \frac{\partial q}{\partial x_1} \tag{6}$$

Plane strain Condition

$$g_1 = \frac{E(1-v)}{(1-2v)(1+v)} \frac{\varepsilon_{11}^2}{2} \frac{\partial q}{\partial x_1} \tag{7}$$

$$g = \frac{E}{1+v} \varepsilon_{12} \frac{\partial u_2}{\partial x_1} \frac{\partial q}{\partial x_1} \tag{8}$$

$$g_3 = \frac{E}{1+v} \varepsilon_{12} \varepsilon_{11} \frac{\partial q}{\partial x_2} \tag{9}$$

$$g_4 = \frac{E}{(1+v)(1-2v)} ((1-v)\varepsilon_{22} + v\varepsilon_{11}) \frac{\partial u_2}{\partial x_1} \frac{\partial q}{\partial x_2} \tag{10}$$

$$g_5 = \frac{E}{1+v} \varepsilon_{12}^2 \frac{\partial q}{\partial x_1} \tag{11}$$

$$g_6 = \frac{E}{1-v^2} \left(\frac{\varepsilon_{22}^2}{2} (1-v) + v\varepsilon_{11}\varepsilon_{12} \right) \frac{\partial q}{\partial x_1} \tag{12}$$

Appendix-II

Plane stress

$$G_1 = \frac{E}{1-v^2}\frac{\partial q}{\partial x_1}\left[\varepsilon_{11}\frac{\partial \dot{u}_1}{\partial x_1} - \varepsilon_{11}^2\frac{\partial V_1}{\partial x_1}\right] \tag{13}$$

$$G_2 = \frac{E}{1+v}\frac{\partial q}{\partial x_1}\left[\frac{\partial u_2}{\partial x_1}\left(\frac{\partial \dot{u}_2}{\partial x_1} + \frac{1}{2}\frac{\partial \dot{u}_1}{\partial x_1} - \frac{1}{2}\varepsilon_{11}\frac{\partial V_1}{\partial x_2} - \frac{\partial u_2}{\partial x_1}\frac{\partial V_1}{\partial x_1}\right) + \frac{1}{2}\frac{\partial u_1}{\partial x_1}\left(\frac{\partial \dot{u}_1}{\partial x_1} - \frac{\partial u_2}{\partial x_1}\frac{\partial V_1}{\partial x_1}\right)\right] \tag{14}$$

$$G_3 = \frac{1}{2}\frac{E}{1+v}\frac{\partial q}{\partial x_2}\left[\varepsilon_{11}\left(\frac{\partial \dot{u}_2}{\partial x_1} + \frac{\partial \dot{u}_1}{\partial x_2}\right) + 2\varepsilon_{12}\frac{\partial \dot{u}_1}{\partial x_1} - \varepsilon_{11}^2\frac{\partial V_1}{\partial x_2} - \varepsilon_{11}\frac{\partial u_2}{\partial x_1}\frac{\partial V_1}{\partial x_1}\right] - \varepsilon_{11}\varepsilon_{12}\frac{E}{1+v}\frac{\partial q}{\partial x_1}\frac{\partial V_1}{\partial x_2} \tag{15}$$

$$G_4 = \frac{E}{1-v^2}\frac{\partial q}{\partial x_2}\frac{\partial u_2}{\partial x_1}\left(\frac{\partial \dot{u}_2}{\partial x_2} + v\frac{\partial \dot{u}_1}{\partial x_1}\right) - \frac{E}{1-v^2}\frac{\partial q}{\partial x_2}\left[\left(\frac{\partial u_2}{\partial x_1}\right)^2\frac{\partial V_1}{\partial x_2} + v\varepsilon_{11}\frac{\partial u_2}{\partial x_1}\frac{\partial V_1}{\partial x_1}\right] + \frac{E}{1-v^2}(\varepsilon_{22} + v\varepsilon_{11})\left[\frac{\partial q}{\partial x_2}\frac{\partial \dot{u}_2}{\partial x_1} - \frac{\partial q}{\partial x_1}\frac{\partial u_2}{\partial x_1}\frac{\partial V_1}{\partial x_2}\right] \tag{16}$$

$$G_5 = \frac{E}{1+v}\frac{\partial q}{\partial x_1}\varepsilon_{12}\left[\frac{\partial \dot{u}_1}{\partial x_2} + \frac{\partial \dot{u}_2}{\partial x_1} - \frac{\partial u_2}{\partial x_1}\frac{\partial V_1}{\partial x_1} - \varepsilon_{11}\frac{\partial V_1}{\partial x_2}\right] \tag{17}$$

$$G_6 = \frac{E}{1-v^2}\frac{\partial q}{\partial x_1}\left[(\varepsilon_{22} + v\varepsilon_{11})\left(\frac{\partial \dot{u}_2}{\partial x_2} - \frac{\partial u_2}{\partial x_1}\frac{\partial V_1}{\partial x_2}\right) + v\varepsilon_{22}\left(\frac{\partial \dot{u}_2}{\partial x_1} - \varepsilon_{11}\frac{\partial V_1}{\partial x_1}\right)\right] \tag{18}$$

Plane strain

$$G_1 = \frac{E(1-v)}{(1+v)(1-2v)}\frac{\partial q}{\partial x_1}\left[\varepsilon_{11}\frac{\partial \dot{u}_1}{\partial x_1} - \varepsilon_{11}^2\frac{\partial V_1}{\partial x_1}\right] \tag{19}$$

$$G_2 = \frac{E}{1+v}\frac{\partial q}{\partial x_1}\left[\frac{\partial u_2}{\partial x_1}\left(\frac{\partial \dot{u}_2}{\partial x_1} + \frac{1}{2}\frac{\partial \dot{u}_1}{\partial x_1} - \frac{1}{2}\varepsilon_{11}\frac{\partial V_1}{\partial x_2} - \frac{\partial u_2}{\partial x_1}\frac{\partial V_1}{\partial x_1}\right) + \frac{1}{2}\frac{\partial u_1}{\partial x_1}\left(\frac{\partial 2}{\partial x_1} - \frac{\partial u_2}{\partial x_1}\frac{\partial V_1}{\partial x_1}\right)\right] \tag{20}$$

$$G_3 = \frac{1}{2}\frac{E}{1+v}\frac{\partial q}{\partial x_2}\left[\varepsilon_{11}\left(\frac{\partial \dot{u}_2}{\partial x_1} + \frac{\partial \dot{u}_1}{\partial x_2}\right) + 2\varepsilon_{12}\frac{\partial \dot{u}_1}{\partial x_1} - \varepsilon_{11}^2\frac{\partial V_1}{\partial x_2} - \varepsilon_{11}\frac{\partial u_2}{\partial x_1}\frac{\partial V_1}{\partial x_1}\right] - \varepsilon_{11}\varepsilon_{12}\frac{E}{1+v}\frac{\partial q}{\partial x_1}\frac{\partial V_1}{\partial x_2} \tag{21}$$

$$G_4 = \frac{E}{(1+v)(1-2v)}\frac{\partial q}{\partial x_2}\frac{\partial u_2}{\partial x_1}\left[v\left(\frac{\partial \dot{u}_1}{\partial x_1} - \varepsilon_{11}\frac{\partial V_1}{\partial x_1}\right) + (1-v)\left(\frac{\partial \dot{u}_2}{\partial x_2} - \frac{\partial u_2}{\partial x_1}\frac{\partial V_1}{\partial x_2}\right)\right] + \frac{E}{(1+v)(1-2v)}((1-v)\varepsilon_{22} + v\varepsilon_{11})\left[\frac{\partial q}{\partial x_2}\frac{\partial \dot{u}_2}{\partial x_1} - \frac{\partial q}{\partial x_1}\frac{\partial u_2}{\partial x_1}\frac{\partial V_1}{\partial x_2}\right] \tag{22}$$

$$G_5 = \frac{E}{1+v}\frac{\partial q}{\partial x_1}\varepsilon_{12}\left[\frac{\partial \dot{u}_1}{\partial x_2} + \frac{\partial \dot{u}_2}{\partial x_1} - \frac{\partial u_2}{\partial x_1}\frac{\partial V_1}{\partial x_1} - \varepsilon_{11}\frac{\partial V_1}{\partial x_2}\right] \tag{23}$$

$$G_6 = \frac{E}{(1+v)(1-2v)}\frac{\partial q}{\partial x_1}\left[((1-v)\varepsilon_{22} + v\varepsilon_{11})\left(\frac{\partial \dot{u}_2}{\partial x_2} - \frac{\partial u_2}{\partial x_1}\frac{\partial V_1}{\partial x_2}\right) + v\varepsilon_{22}\left(\frac{\partial \dot{u}_2}{\partial x_1} - \varepsilon_{11}\frac{\partial V_1}{\partial x_1}\right)\right] \tag{24}$$

Appendix-III

Start

Input Subroutine

Calculation of stiffness matrix

(Calculation of stiffness matrix depend upon the type of element)

Type of eleme

Blending

Blending stiffness matrix

Assembly of Global stiffness

Enriched Element

Enriched stiffness matrix

Assembly of Global stiffness

Classical Element

Classical stiffness matrix

Assembly of Global stiffness

Modification for Boundary Conditions

(Using Penality Approach)

Solving the system of discrete linear equations

(Using least square approach)

A

```
            ( A )
              |
              |
              v
    +---------------------------+
    |   Reaction Calculation    |
    +---------------------------+
              |
              v
    +---------------------------+
    |     Stress Calculation    |
    +---------------------------+
              |
              v
    +------------------------------------+
    | Stress smoothing and Nodal averaging |
    +------------------------------------+
              |
              v
    +---------------------------+
    |  Plotting Stress Results  |
    +---------------------------+
              |
              v
    +---------------------------+
    |      SIF Calculation      |
    +---------------------------+
              |
              v
    +----------------------------------------------+
    | Calculation of J-Integral and Energy density |
    +----------------------------------------------+
              |
              v
           (  End  )
```

Structure of GFEM code for fracture problem

Brief description of code and its subroutine:

The main GFEM code contains different subroutines such as inputData, Stiffness matrix, solver, and various post processing subroutines (i.e. Stress calculation SIF calculation, J-Integral calculation and many more). Main program execute the subroutine as per the algorithm of Classical finite element method. It makes the difference from classical FEM in the calculation of stiffness matrix. Calculation of stiffness matrix depends upon the shape function derivative matrix. In case of GFEM, shape function derivative matrix becomes 3*48 in size while it was 3*8 in Classical FEM. Following sub section will give brief introduction about each subroutine.

1. **InputData:** This subroutine reads the input file and stores the data with a specific variable name. this subroutine reads the following data

   a. Mesh data- (Node numbers, Element numbers, Number of Material, Number of dimensions, Node per element and others relevant information)

   b. Connectivity matrix of mesh

   c. Nodal coordinate

   d. Material properties

   e. Boundary conditions

   f. Applied Force

   g. Crack information

2. **Stiffness Matrix Subroutine:** In GEFM, there are three types of element (i.e. 1.Classical Element 2. Enriched Element, 3. Blending element). Depending on the type of element this subroutine calls the other subroutines.

   a. **Classical Element Stiffness matrix**: This subroutine is very similar to Classical FEM stiffness calculation and assembly. It gives the element stiffness matrix of size 8*8 and after assembly it gives in the same size that of global stiffness matrix.

   b. **Enriched Element Stiffness matrix**: This subroutine become little tough to handle. Size of stiffness matrix increases from 8*8 to 48*48 depending upon the type and numbers of enrichment function. This subroutine matrix calls the B matrix (Derivative of shape function) subroutine. Shape function derivative matrix becomes of size 3*48. This comprises of B matrix from Heaviside enrichment and crack tip enrichment function.

Each enrichment function gives a 3*8 size matrix. If there are 5 enrichment functions then the size of B matrix becomes 3*48.

c. **Blending Element Stiffness matrix**: this subroutine works in the same lines as the enrichment subroutine works. This subroutine is having addition Ramp function which varies from 0 to 1. This ramp function ensures the continuity of the displacement approximation.

Assembly of Global Stiffness matrix: Assembly is similar to classical finite element method procedure. In case of blending and enrichment function we have some additional dofs, which are tricky to assemble. In this code, I have assigned a phantom number to each additional dof. This phantom numbers starts after the actual node number finished. These numbers helps in placing the additional dofs in a known position.

3. **Modification of Boundary conditions:** This subroutine is based on the penality approach. Global stiffness matrix is modified for the given prescribed boundary conditions.

4. **Solve:** In this subroutine the linear system of equation are solved. This subroutine uses the least square method to find out the solution of linear system of equations. This subroutine first check about the consistency of linear system of equation. If the system is not consistent, then it gives the massage about same as warning.

5. **Reaction calculation:** When the system of linear equation vas been solved. Using the displacement field, we have cacluated the reaction for each degree of freedom which was given as prescribed boundary condition.

6. **Stress Calclulation:** Now the displacement and all the reactions are known to us. Using the displacement field this subroutine calculates the stress field. This subroutine recall the B matrix subroutine and needs the displcement vector as the input. As the output it gives the stress at all the Gauss points.

7. **Stress Smoothing and Nodal Averaging:** Stress calculation subroutine gives the stress value at all the gauss point, where required output is stresses value at all the Nodal points. For the same objective, gauss point stress values are mapped to the nodal point using the mass matrix concept. When we got the Nodal value, we did the nodal averaging for getting the exact nodal stress value. This subroutine is limited to the arithmetic averaging but advisable method is weighted averaging. Weighted averaging gives a better picture of stress distribution.

8. **Plot Results:** MATLAB is good plotting tool but we have to be little care full while defining the axix variables as well as the format of data. In this subroutine we are converting vector data into the matrix form so that contour plotting can be done very easily. This subroutine needs the sorting also, when our mesh is randomly generated. It gives a message for that.

9. **Fracture Parameter calculation:** This is collection of different subroutine, which contains the calculation of the SIF, J-Integral separately. On the requirement this subroutine can be changed. It's the flexibility given to the user.

References

[1] T. Belystchko, T.Black. "Elastic crack growth in finite element with minimal remeshing", International Journal for numerical methods in Engineering; 45(5), pp.601-620, 1999.

[2] J.M.Melnek, I.Babuska, "The partition of unity finite element method", Computer Methods in Applied Mechanics and Engineering 139, pp 289-314, 1996.

[3] T Strouboulis, K Copps, I.Babuska, "The design and analysis of the generalized finite element method, Computer methods Appl Mechancis and Engineering, 181 (1) , pp 43-69, 2000.

[4] T Strouboulis, K Copps, I.Babuska, "The generalized finite element method", Computer Methods in Applied Mechanics and Engineering 190, pp. 4081-4193, 2001.

[5] C.A. Duarte, D-J. Kim, "Analysis and application of a generalized finite element method with global-local enrichment functions", Computer methods in Applied Mechanics and Engineering 197, pp. 487-504, 2008.

[6] S.Mohammadi 'EXTENDED FINITE ELEMENT METHOD for fracture analysis of structures', Blackwell Publishing, 2008.

[7] Belytschko, T., Xu, J.X., Chessa, J., Moës, N. and Gravouil, A. Recent developments in meshless and extended finite element methods. Second International Conference on Advanced Computational Methods in Engineering, Eindhoven, The Netherlands. 2002b.

[8] T.Fries, T. Belytschko " The intrinsic X-FEM: a method for arbitrary discontinuities without additional unkowns", International Journal for Numerical Methods in Engineering, 68, pp 1358-1385, 2006

[9] S.E. Mousavi, E.Grinspun and N.Sukumar "Higher order extended finite element with harmonic enrichment functions for complex crack problem", International Journal of Numerical Methods in Engineering, 00, pp 1-29, 2010

[10] W.Aquino, J.C. Brigham, C.J. Earls, N.Sukumar "Generalized finite element using proper orthogonal decomposition", International Journal for numerical Method in Engineering, 79(7), pp. 887-906, 2010.

[11] N.Moess, M Cloirec, P. Cartraud, J.F.Remacle, " A Computational approach to handle the complex microstructure geometries", Computer Method in Applied Mechanics and Enggs, 192 pp 3163-3177, 2003.

[12] M.Arndt, R.D.Machado, A.Scremin "An Adaptive generalized finite element method applied to free vibration analysis of the straight bars and trusses", Journals of sound and vibration, 329 pp 659-672, 2010.

[13] G. Ventura "On the elimination of quadrature subcells for discontinuous functions in the extended finite-element method" . International Journal for Numerical Methods in Engineering, 66, pp. 761–795, 2006.

[14] P. Laborde, Pommier, J., Renard, Y. and M. Salaün, " High-order extended finite element method for cracked domains'. International Journal for Numerical Methods in Engineering, 64, pp 354–381, 2005.

[15] E. Chahine, P. Laborde. and Y. Renard, " A quasi-optimal convergence result for fracture mechanics with XFEM". Academie des Sciences, Paris, Ser. I 342, pp. 527–532, 2006.

[16] M. Peters, and K. Hack, "Numerical aspects of the extended finite element method'. Proceedings of Applied Mathematics and Mechanics, 5, pp. 355–356, 2005.

[17] Q. Z. Xiao, and B.L. Karihaloo, "Improving the accuracy of XFEM crack tip fields using higher order quadrature and statically admissible stress recovery". International Journal for Numerical Methods in Engineering, 66, pp. 1378–1410, 2006.

[18] I. Hirari, Y. Uchiyama, Y. Mizuta, and W.D. Pilkey, "An exact zooming method". Finite Elements in Analysis and Design, 1, pp. 61–69, 1985.

[19] K. Haidar, J.F.Dube, and G.Pijaudier-Cabot, "Modelling crack propagation in concrete structures with a two scale approach". International Journal for Numerical and Analytical Methods in Geomechanics, 27, pp. 1187–1205, 2003.

[20] P.M.A. Areias, and T. Belytschko, "Non-linear analysis of shells with arbitrary evolving cracks using XFEM". International Journal for Numerical Methods in Engineering, 62, pp. 384–415, 2005.

[21] P.M.A. Areias, J.H. Song, and T.Belytschko, "Analysis of fracture in thin shells by overlapping paired elements". Computer Methods in Applied Mechanics and Engineering, 195, pp. 5343–5360, 2006.

[22] A. Hansbo , P. Hansbo , "a finite element method for simulation of strong and weak discontinuity in solid mechancs", Computer Methods in Applied Mechanics and Engineering, 193, pp. 3523-3540, 2004.

[23] T. Belytschko, H.Chen, J.Xu, and G. Zi,"Dynamic crack propagation based on loss of hyperbolicity and a new discontinuous enrichment". International Journal for Numerical Methods in Engineering, 58, pp. 1873–1905, 2003

[24] T. Belytschko, and H. Chen, "Singular enrichment finite element method for elastodynamic crack propagation". International Journal of Computational Methods, 1 (1), pp. 1–15, 2004.

[25] G. Zi, H. Chen, J. Xu, and T. Belytschko, "The extended finite element method for dynamic fractures". Shock and Vibration, 12, 9–23, 2005.

[26] J. Réthoré, A. Gravouil, and A. Combescure, "An energy-conserving scheme for dynamic crack growth using the extended finite element method". International Journal for Numerical Methods in Engineering, 63, 631–659, 2005a.

[27] T. Menouillard, J. Réthoré, A. Combescure and H. Bung, " Efficient explicit time stepping for the extended finite element method (X-FEM)". International Journal for Numerical Methods in Engineering, 68 (9), pp.911–939, 2006.

[28] J. Chessa, and T. Belytschko, "Arbitrary discontinuities in space–time finite elements by level sets and X-FEM". International Journal for Numerical Methods in Engineering, 61, pp. 2595–2614, 2004.

[29] J. Chessa, and T. Belytschko, "A local space–time discontinuous finite element method". Computer Methods in Applied Mechanics and Engineering, 195, pp. 1325–1343, 2006.

[30] J. Réthoré, A. Gravouil, and A.Combescure, "A combined space–time extended finite element method". International Journal for Numerical Methods in Engineering, 64, 260–284, 2005b.

[31] I. Babuska, U. Banerjee, J.E. Osborn, " On the principle for the selection of shape functions for the Generalized finite element method:, 191 pp. 5595-5629, 2002

[32] J. Chessa, H.Wang, T. Belytschko, " On the construction of blending element for local partition of unity enriched finite elements", International Journal for numerical methods in engineering, 57, pp. 1015-1038, 2003

[33] I. Babuska, Uday Banerjee, J.E. Osborn, " Generalized finite element methods- main ideas, results and perspective", International journal of computation methods, 1, pp. 67-103, 2004

[34] J.P. Pereira, C.A. Duarte, " Extraction of stress intensity factors from generalized finite element solutions", 29, pp. 397-413, 2005

[35] T. Strouboulis, I. Babuska, R. Hidajat, "The Generalized finite element method for Helmholtz equation: Theory, computation, and open problems", Computer methods in applied mechanics and engineering, 195, pp. 4711-4731, 2006

[36] T. Strouboulis, R. Hidajat, I. Babuska,,"The Generalized finite element method for Helmholtz equation. Part II: Effects of choice of handbook functions, error due to absorbing boundary conditions and its assessment", Computer methods in applied mechanics and engineering, 197, pp. 364-380, 2008

[37] C.A. Duarte, D.J. Kim, "Analysis and design of a generalized finite element method with global-local enrichment functions", Computer methods in applied mechanics, and engineering, 197, pp. 487-504, 2008

[38] K.R. Srinivasan, K. Matous, P.H. geubelle, " Generalized finite element method for modelling nearly incompressible biomaterial hyperplastic solids", Computer methods in applied mechanics and engineering, 197, pp. 4882-4893, 2008

[39] T. Belystchko , R. Gracie G. Ventura, " A review of extended/generalized finite element methods for material modelling", Modelling and simulation in material science and engineering, 17, pp. abc-xyz, 2009

[40] M. Arndt, R.D. Machado, A.Scremin, "An adaptive generalized finite element method applied to free vibration analysis of straight bars and trusses" , Journal of sound and vibrations 329, pp. 659-6672, 2010

[41] I. Babuska, R. Lipton, " Optimal local approximation spaces for the generalized finite element methods with application to multiscale problems", Multiscale modelling and simulation, 9(1), pp. 373-406, 2011

[42] G.Bugeda, J.Oliver , "A general methodology for structural shape optimization problems using automatic adaptive remeshing". International journal of numerical methods in engineering, 36 (18), pp. 3161-3185, 1993.

[43] G.H. Paulino, F. Shi, S.Mukherjee, P.Ramesh, "Nodal sensitivities as error estimate in computation mechanics", Acta Mecahnica, 121 pp. 191-213, 1997.

[44] K. Washizu, "Variational methods in Elasticity and Plasticity", Pergamon Press, NewYork, 1968.

[45] J.D.Logan, "Invariant variational principles in mathematics in science and engineering, Academic Press New York, 1977.

[46] E.Taroco, "Shape sensitivity analysis in linear elastic facture mechanics", Computer methods in applied mechanics and engineering, 188, pp. 697-712, 2000.

[47] G. Chen, S. Rahman, Y.H. Park, " Shape sensitivity analysis of linear elastic cracked structures under Mode-I loading", Journal of pressure vessel technology, 124, pp. 476-482, 2002

[48] S. Rahman, B.N.Rao,"Continuum shape sensitivity analysis of the mode –I fracture in functionally graded materials", computer mechanics, 36, pp. 62-75, 2005.

[49] M.S. Edke, K.H. Chang, "Shape sensitivity analysis for 2-D mixed mode fractures using XFEM and level set method", Mechanics based design of structure and machines, 38,pp. 328-347, 2010.

[50] Choi KK, Chang KH, " A study of design velocity field computation for shape optimal design", finite element analysis and design, 15(4), pp. 317-341, 1994

[51] Haug.E.J., Choio. K.K. Komkov V. "Design sensitivity analysis of structure systems", Academic press New York, 1986.

[52] N. Sukumar N, DL. Chopp , N. Mo¨es , T. Belytschko "Modeling holes and inclusions by level sets in the extended finite-element method", Computer Methods in Applied Mechanics and Engineering 190, pp.6183–6200, 2001

[53] Robert Gracie, Hongwu Wang and Ted Belytschko "Blending in the extended finite element method by discontinuous Galerkin and assumed strain methods", Int. J. Numer. Meth. Engng 74, pp. 1645–1669, 2008

[54] W.H. Reed, T.R.Hill. "Triangular mesh methods for the neutron transport equation", Los Alamos Scientific Laboratory Report LA-UR-73-479, 1973

[55] T. Fries "A corrected XFEM approximation without problems in blending elements", International Journal for Numerical Methods in Engineering, DOI: 10.1002/nme.2259, 2007

[56] J.E. Dolbow, " An extended finite element method with discontinuous enrichment for applied mechanics", PhD thesis, Theoretical and Applied Mechanics, Northwestern University, USA